Soil Dynamics and Earthquake Engineering 81 (2016) 42–57

Contents lists available at ScienceDirect

Soil Dynamics and Earthquake Engineering

journal homepage: www.elsevier.com/locate/soildyn

Analytical solution of the asymmetric transient wave in a transversely isotropic half-space due to both buried and surface impulses

Mehdi Raoofian Naeeni [a], Morteza Eskandari-Ghadi [b,*]

[a] Faculty of Geomatics Engineering, Department of Geodesy, K. N. Toosi University of Technology, Iran
[b] School of Civil Engineering, College of Engineering, University of Tehran, Iran

ARTICLE INFO

Article history:
Received 25 August 2015
Received in revised form
10 November 2015
Accepted 12 November 2015
Available online 4 December 2015

Keywords:
Transient waves
Transversely isotropic half-space
Potential functions
Joint Hankel–Laplace transform

ABSTRACT

With the aid of a complete set of two scalar potential functions, the problem of transient wave propagation in transversely isotropic half-space, subjected to time dependent tractions applied on a finite patch at an arbitrary depth below the free surface of the half-space is investigated. With the use of the displacement–potential function relationships in a cylindrical coordinate system, the coupled equations of motion are uncoupled; resulting in two separate partial differential equations one of which is second order and the other is fourth order. These two partial differential equations are solved with the aid of both Fourier series expansion and joint Hankel–Laplace integral transforms. The solutions are also investigated in details for tractions varying with time as Heaviside step function, which may be used as a kernel in any integral based method for more complicated elastodynamic initial-boundary value problems. Moreover, some displacement Green's functions are numerically evaluated for a synthetic transversely isotropic material to graphically demonstrate the transient motion of the free surface of the half-space.

1. Introduction

Because of its applications and mathematical challenges, both engineers and mathematicians are interested in the wave propagation in elastic solids especially in a time domain (see for example [1,2]). The study of elastic wave propagation, particularly those with transient nature, has many applications in linear and nonlinear soil–structure-interaction, foundation analysis including piles and underground structures [3], dynamic compaction of soil, dynamic replacement of soil, Earthquake engineering, foundation of theoretical seismology, geophysical related problems and machine foundation design [4–9]. The fundamental solutions for transient elastodynamics of either full-space or half-space may be used for integral base numerical solution of nonlinear soil–structure interaction for more complicated geometry [10,3]. Analytical solutions play an important role in a deep understanding of a scientific phenomenon [11,12], although some simplifications need to be made in the process of deriving them. In particular, analytical solutions can also play a unique role in validating many new numerical methods [13,14]. For these reasons, analytical solutions have been derived in recent years for many scientific problems. In actual engineering problems, where the effects of complex loading situation and complex boundary conditions are indispensable, the numerical methods must be used to solve the problem. One of the powerful numerical methods for solving the linear partial differential equations arise in engineering problems is the boundary element method (BEM), where analytical solution in the domain is, (with the aid of Betti's theorem [4]), obtained after determining the values of the interested fields at the boundary, numerically [10,3]. However, this method needs the determination of the Green's functions for the problem associated with the boundary conditions. Thus in the recent years, a lot of researches have been devoted for determination of Green's functions. Rajapakse and Wang [15], with the use of displacement potential function accompanied with Fourier transform determined the dynamic displacement Green's functions of an orthotropic elastic half-plane subjected to a time-harmonic buried force. Wang and Rajapakse [16] found the internal source Green's function for a transversely isotropic half-space in a time domain in both 2D and 3D cases, where the joint of Laplace–Fourier and Laplace–Hankel integral transforms were used, respectively for 2D and 3D states after using a displacement potential functions for the equations of motion. Wang and Achenbach [17] determined both the 3D and 2D time-domain elastodynamic Green's functions for linearly elastic anisotropic materials with the application of Radon transform. Their fundamental solutions are in the form of a surface integral over the surface of a unit sphere for 3-D cases and

* Corresponding author.
E-mail addresses: mraoofian@kntu.ac.ir (M. Raoofian Naeeni), ghadi@ut.ac.ir (M. Eskandari-Ghadi).

http://dx.doi.org/10.1016/j.soildyn.2015.11.003
0267-7261/

are over a unit circle path for 2D cases. In addition, their Green's functions are evaluated in the frequency domain readily by a subsequent evaluation of the Fourier transforms of the time-domain solutions. Kausel [18] presented the Green's functions for many different cases such as SH line load, double couples, suddenly line and point loads, etc.

One of the most important contributions in the analytical study of transient wave propagation in elastic isotropic materials is due to Pekeris [19–21]. With the aid of the Laplace and Hankel integral transforms, implementation of Helmholtz decomposition theorem, and the use of Cagniard-De Hoop trick [22,23], Pekeris [21,22] derived an analytical solution for the transient equations of motion in an axisymmetric half-space due to surface and buried impulse loading. In particular, he computed the displacement at the free surface and showed the arrival time of different waves including $P-$, $SV-$ and Rayleigh waves. Chao [24] derived a closed form solution for radial and tangential displacements at the surface of a half-space due to surface horizontal point force varying with time as a Heaviside step function. Jin and Liu [25], with the use of the joint Hankel–Laplace integral transforms accompanied with Cagniard–De Hoop method, have determined the exact analytical solution for the horizontal displacement at the center of a circular surface patch of an elastic isotropic half-space, which is under an impulsive constant distributed loading.

Anisotropy is a common property of engineering materials such as soil (because of sedimentation), rock, reinforced concrete and many man-made materials such as composites and piezo-composites. Thus, the wave propagation in anisotropic materials is recently of major concern. The high performance of anisotropic materials in technological applications is another reason for studying the response of anisotropic material to mechanical force, displacement and other phenomenon. Most innovative materials such as composites, piezo-composites and magnetics are anisotropic, and in applications need to be modeled as either transversely isotropic or orthotropic materials [26,27]. The early work of Stoneley [28] revealed that wave propagation in a transversely isotropic medium gives rise to a phenomenon, which greatly differs from the case where the medium is isotropic. Later, Synge [29], Buchwald [30] and Payton [31] studied the elastodynamic problems pertinent to the transversely isotropic half-space.

The potential method is a powerful tool for solving the coupled both equilibrium equations and equations of motion. Lekhnitskii in 1940 derived a potential function for axisymmetric elastostatic problems of transversely isotropic media [32,33]. Hu [34] and Nowakii [35] studied the general case of elastostatic problem in transversely isotropic media and generalized Lekhnitskii's solution to the asymmetric case, which is now called as Lekhnitskii–Hu–Nowacki solution [36]. Eskandari-Ghadi [33] has introduced a complete solution for the general elastodynamics problems in linear transversely isotropic mono-axial-convex domain in terms of two potential functions, one of which describes *SH*-wave and the other gives both *SV*- and *P*-waves in any plane containing the axis of material symmetry. With the aid of this representation, Eskandari-Ghadi and Sattar [37], investigated the problem of transient wave in an axisymmetric transversely isotropic half-space due to surface loading and their solution included an integral representation with a finite limit.

In the present study, a transversely isotropic half-space is considered as the domain of the problem, and the potential functions introduced by Eskandari-Ghadi [33] is implemented to derive the analytical solution for the displacement Green's function of transversely isotropic half-space under the action of transient tractions applied at an arbitrary depth of the half-space. To do so, with the use of the representations for the displacements, in terms of two scalar potential functions; the elastodynamic governing partial differential equations are uncoupled into a fourth- and a second-order partial differential equations in cylindrical coordinate system and solved by virtue of Fourier series expansion in terms of the angular coordinate and joint Hankel–Laplace integral transforms in term of radial-time variables, along with satisfying both the boundary and regularity conditions.

The Green's functions derived in this paper are applicable as integral kernels in the boundary element method or any other boundary integral formulations to solve more complicated engineering initial-boundary value problems such as either linear or non-linear dynamic analysis of anisotropic soil–structure-interaction as well as earthquake engineering and rock engineering relevant problems. For instance, the topic of the forced vibrations of rigid disc embedded at an arbitrary depth in a semi-infinite transversely isotropic medium, which is a subject of considerable interest in geo-mechanics and civil engineering could be treated with the aid of these Greens' functions [38,39]. Another interesting application of the proposed model may be found in geophysical applications, such as earthquake and volcano source monitoring. Moreover, the Green's functions for the point load excitation may be used in the dislocation formulation of co-seismic deformations arise from the rupture of buried faults, so that they can find some applications in the emerging computational geosciences field [40–43].

2. Statement of the problem

A transversely isotropic half-space in a cylindrical coordinate system is considered as the domain of the problem in such a way that the axis of symmetry of the material to be depth-wise (Fig. 1). The displacement equations of motion in the cylindrical coordinate system for homogenous transversely isotropic solid in the absence of body force may be expressed as [26]:

$$C_{11}\left(\frac{\partial^2 u}{\partial r^2}+\frac{1}{r}\frac{\partial u}{\partial r}-\frac{u}{r^2}\right)+C_{66}\frac{1}{r^2}\frac{\partial^2 u}{\partial \theta^2}+C_{44}\frac{\partial^2 u}{\partial z^2}-(C_{11}+C_{66})\frac{1}{r^2}\frac{\partial v}{\partial \theta}$$
$$+(C_{12}+C_{66})\frac{1}{r}\frac{\partial^2 v}{\partial r\partial \theta}+(C_{13}+C_{44})\frac{\partial^2 w}{\partial r\partial z}=\rho\frac{\partial^2 u}{\partial t^2}, \tag{1}$$

$$C_{66}\left(\frac{\partial^2 v}{\partial r^2}+\frac{1}{r}\frac{\partial v}{\partial r}-\frac{v}{r^2}\right)+C_{11}\frac{1}{r^2}\frac{\partial^2 v}{\partial \theta^2}+C_{44}\frac{\partial^2 v}{\partial z^2}+(C_{13}+C_{44})\frac{\partial^2 w}{\partial \theta\partial z}$$
$$+(C_{12}+C_{66})\frac{1}{r}\frac{\partial^2 u}{\partial r\partial \theta}+(C_{11}+C_{66})\frac{1}{r^2}\frac{\partial u}{\partial \theta}=\rho\frac{\partial^2 v}{\partial t^2}, \tag{2}$$

$$C_{44}\left(\frac{\partial^2 w}{\partial r^2}+\frac{1}{r}\frac{\partial w}{\partial r}+\frac{1}{r^2}\frac{\partial^2 w}{\partial \theta^2}\right)+(C_{13}+C_{44})\left(\frac{\partial^2 u}{\partial r\partial z}+\frac{1}{r}\frac{\partial u}{\partial z}+\frac{1}{r}\frac{\partial^2 v}{\partial \theta\,\partial z}\right)$$
$$+C_{33}\frac{\partial^2 w}{\partial z^2}=\rho\frac{\partial^2 w}{\partial t^2}, \tag{3}$$

where $\mathbf{u}=(u,v,w)$ is the displacement vector, C_{11}, C_{33}, C_{12}, C_{13}, C_{44} and $C_{66}=(C_{11}-C_{12})/2$ are the elastic constants and ρ is the density of the medium. In view of the positive definiteness of the

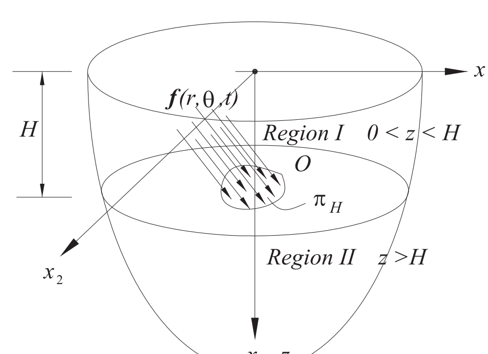

Fig. 1. Transversely isotropic half-space under buried arbitrary time dependent force.

strain energy, the elastic constants should satisfy the following inequalities [44].

$$C_{11}>0, C_{33}>0, C_{66}>0, C_{11}C_{33}-C_{13}^2-C_{33}C_{66}>0. \tag{4}$$

It is assumed that the medium is at rest prior to the instant $t=0$, thus the displacement and stress components are zeros at $t\le 0$. An arbitrary traction, $\mathbf{f}(r,\theta,t)$, is assumed to be distributed on a finite patch π_H located at depth $z=H$ (see Fig. 1). Thus, the prescribed boundary conditions at $z=H$ are

$$-S_{zr}(r,\theta,H^+,t)+S_{zr}(r,\theta,H^-,t)=\begin{cases}P(r,\theta,t) & r,\theta\in\pi_H\\ 0 & r,\theta\notin\pi_H\end{cases},$$
$$-S_{zz}(r,\theta,H^+,t)+S_{zz}(r,\theta,H^-,t)=\begin{cases}R(r,\theta,t) & r,\theta\in\pi_H\\ 0 & r,\theta\notin\pi_H\end{cases},$$
$$-S_{z\theta}(r,\theta,H^+,t)+S_{z\theta}(r,\theta,H^-,t)=\begin{cases}Q(r,\theta,t) & r,\theta\in\pi_H\\ 0 & r,\theta\notin\pi_H\end{cases} \tag{5}$$

where S_{ij} $(i,\ j=r,\ z,\theta)$ are the components of stress tensor and P, Q and R are the components of the known traction in radial, angular and vertical directions, respectively. In addition, the displacements and stresses have to obey the regularity conditions at infinity.

According to Eskandari-Ghadi (2005), the complete solution of Eqs. (1)–(3) in a z-convex transversely isotropic medium, with a z-axis to be the axis of material symmetry, could be expressed in terms of two scalar potential functions, namely $F(r,\theta,z,t)$ and $\chi(r,\theta,z,t)$ as:

$$u(r,\theta,z,t)=-\alpha_3\frac{\partial^2F(r,\theta,z,t)}{\partial r\partial z}-\frac{1}{r}\frac{\partial\chi(r,\theta,z,t)}{\partial\theta},$$
$$v(r,\theta,z,t)=-\frac{\alpha_3}{r}\frac{\partial^2F(r,\theta,z,t)}{\partial\theta\partial z}+\frac{\partial\chi(r,\theta,z,t)}{\partial r},$$
$$w(r,\theta,z,t)=(1+\alpha_1)\left(\nabla_{r\theta}^2+\frac{\alpha_2}{1+\alpha_1}\frac{\partial^2}{\partial z^2}-\frac{\rho_0}{1+\alpha_1}\frac{\partial^2}{\partial t^2}\right)F(r,\theta,z,t), \tag{6}$$

where

$$\nabla_{r\theta}^2=\frac{\partial^2}{\partial r^2}+\frac{1}{r}\frac{\partial}{\partial r}+\frac{1}{r^2}\frac{\partial^2}{\partial\theta^2}.$$
$$\rho_0=\frac{\rho}{C_{66}}, \alpha_1=\frac{C_{66}+C_{12}}{C_{66}}, \alpha_2=\frac{C_{44}}{C_{66}}, \alpha_3=\frac{C_{13}+C_{44}}{C_{66}} \tag{7}$$

Substituting (6) into the equation of motions, results in two separate partial differential equations (PDEs) governing the equations for the potential functions F and χ as

$$(1+\alpha_1)\left(\Box_1\Box_2-\delta\frac{\partial^4}{\partial z^2\partial t^2}\right)F=0$$
$$\Box_0\chi(r,\theta,z,t)=0. \tag{8}$$

in which

$$\Box_0=\nabla_{r\theta}^2+\alpha_2\frac{\partial^2}{\partial z^2}-\rho_0\frac{\partial^2}{\partial t^2},\quad \Box_1=\nabla_{r\theta}^2+\frac{1}{s_1^2}\frac{\partial^2}{\partial z^2}-\frac{\rho_0}{1+\alpha_1}\frac{\partial^2}{\partial t^2},$$
$$\Box_2=\nabla_{r\theta}^2+\frac{1}{s_2^2}\frac{\partial^2}{\partial z^2}-\frac{\rho_0}{\alpha_2}\frac{\partial^2}{\partial t^2},\ \delta=\frac{\rho_0}{1+\alpha_1}\left(1-\frac{1}{s_1^2}\right)+\frac{\rho_0}{\alpha_2}\left(\frac{\alpha_4}{1+\alpha_1}-\frac{1}{s_1^2}\right),$$
$$\alpha_4=\frac{C_{33}}{C_{66}}. \tag{9}$$

The quantities $s_\alpha^2(\alpha=1,2)$, which are not zero or negative, are the roots of the following equation [44]:

$$C_{33}C_{44}s^4+(C_{13}^2+2C_{13}c_{44}-C_{11}C_{33})s^2+C_{11}C_{44}=0 \tag{10}$$

In view of (4), s_1^2 and s_2^2 can be real and distinct, coalescent, or conjugate complex, however, they cannot be pure imaginary numbers [44].

By considering the Fourier series expansion in terms of angular coordinate and Hankel–Laplace integral transform with respect to radial coordinate and time, respectively, Eq. (8) may be written as an ordinary differential equation in terms of depth. To derive the solution of the resulting equations, it is convenient to view the half-space as being composed of an upper and a lower region of the same material, namely Region **I** $\{0<z<H\}$ and Region **II**$\{z>H\}$, respectively. Consistent with the regularity condition at infinity the general solutions of Eq. (8) in transformed domain may be written as:

$$\bar{\tilde{F}}_m^m=A_m^{\mathbf{I}}e^{\lambda_1z}+B_m^{\mathbf{I}}e^{-\lambda_1z}+C_m^{\mathbf{I}}e^{\lambda_2z}+D_m^{\mathbf{I}}e^{-\lambda_2z},\quad \bar{\tilde{\chi}}_m^m=E_m^{\mathbf{I}}e^{\nu z}+F_m^{\mathbf{I}}e^{-\nu z} \tag{11}$$

for Region **I** and

$$\bar{\tilde{F}}_m^m=B_m^{\mathbf{II}}e^{-\lambda_1z}+D_m^{\mathbf{II}}e^{-\lambda_2z},\quad \bar{\tilde{\chi}}_m^m=F_m^{\mathbf{II}}e^{-\nu z} \tag{12}$$

for Region **II**. In the above equations, $A_m^I,\dots,F_m^I$, B_m^{II}, D_m^{II} and F_m^{II} are constants due to integrations, which are functions of Laplace transform parameter, p, Hankel transform parameter ξ, and elastic coefficients to be determined using the boundary conditions. In the above equations

$$\lambda_1=\sqrt{k_1\xi^2+k_2p^2+\frac{1}{2}\sqrt{k_3\xi^4+k_4\xi^2p^2+k_5p^4}},\quad \nu=\frac{1}{\sqrt{\alpha_2}}\sqrt{\xi^2+\rho_0p^2},$$
$$\lambda_2=\sqrt{k_1\xi^2+k_2p^2-\frac{1}{2}\sqrt{k_3\xi^4+k_4\xi^2p^2+k_5p^4}} \tag{13}$$

with

$$k_1=\frac{1}{2}(s_1^2+s_2^2), k_2=\frac{1}{2}\rho\left(\frac{1}{C_{33}}+\frac{1}{C_{44}}\right), k_3=(s_2^2-s_1^2)^2,$$
$$k_4=2\rho\left[\left(\frac{1}{C_{33}}+\frac{1}{C_{44}}\right)(s_1^2+s_2^2)-2\frac{C_{11}}{C_{33}}\left(\frac{1}{C_{11}}+\frac{1}{C_{44}}\right)\right].k_5=\rho^2\left(\frac{1}{C_{33}}-\frac{1}{C_{44}}\right)^2. \tag{14}$$

Chadwick and Seat [45] showed that three different body waves with different velocities can propagate in each direction in anisotropic elastic materials. However, while the associated displacement vectors are mutually perpendicular to each other, the waves cannot in general be classified into dilatational and rotational types. For transversely isotropic materials one of the body waves is always purely transverse, and since this wave is polarized in planes perpendicular to the direction of symmetry, it may appropriately be referred to as an $SH-$wave. The $SH-$wave number corresponds to the branch point of the function ν and may be expressed as:

$$\xi_{SH}=\pm ip\sqrt{\rho/c_{66}}\,. \tag{15}$$

The other two body waves are called quasi-longitudinal (QL) and quasi-transverse (QT), the former being the wave for which the inclination of the displacement vector to the wave normal is least. However, in principal directions which are corresponding to the eigen-vectors of the acoustic tensor [46], there are two waves, which have pure dilatational (P-wave) and pure transverse behavior (SV-wave). The wave numbers related to these dilatational and transverse waves are the branch points of the functions λ_1 and λ_2, which may be expressed as:

$$\xi_P=\pm ip\sqrt{\rho_0/(1+\alpha_1)}, \xi_{SV}=\pm ip\sqrt{\rho_0/\alpha_2}, \tag{16}$$

Using the transformed displacement and stress potential function relationships [37,47] and considering, the conditions (5) together with the continuity of displacements across the plane $z=H$ and the traction free conditions at the surface $z=0$, provide nine equations required for the solution of the nine unknown coefficients $A_m^I,\dots,F_m^{II}$. Substituting these coefficients into the relations (11) and (12) and with the use of displacement–potential functions relationships and the inverse theorem for Laplace–Hankel integral transforms, the displacements component could

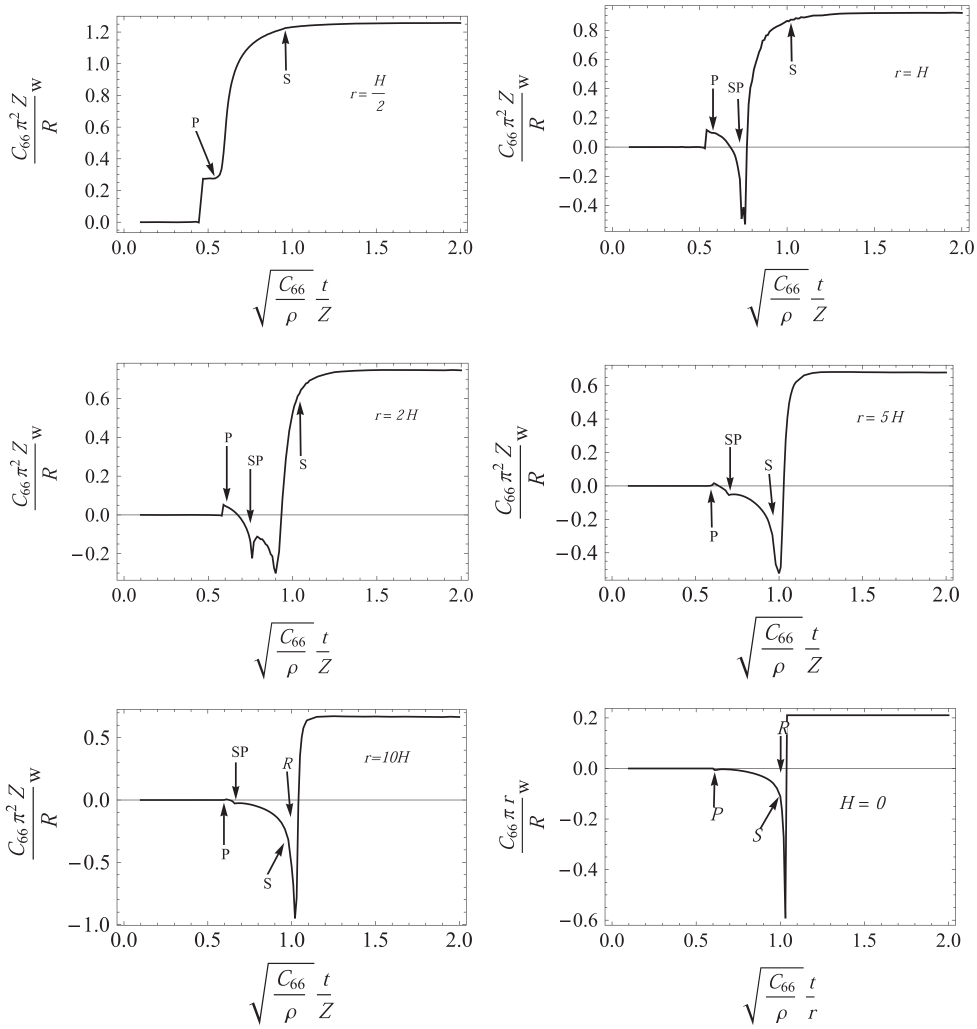

Fig. 2. Surface vertical displacement due to buried vertical point force at different epicenteral distance.

be determined in a real domain as:

$$u(r,\theta,z,t)=\frac{1}{2}\sum_m\left\{\frac{1}{2\pi i}\int_0^\infty e^{pt}\left[\int_0^\infty \xi\left(\gamma_1\left(\frac{X_m-Y_m}{2c_{44}}\right)+\gamma_2\left(\frac{X_m+Y_m}{2c_{44}}\right)+\gamma_3\left(\frac{Z_m}{c_{44}}\right)\right)J_{m-1}(\xi r)d\xi+\int_0^\infty \xi\left(-\gamma_1\left(\frac{X_m-Y_m}{2c_{44}}\right)+\gamma_2\left(\frac{X_m+Y_m}{2c_{44}}\right)-\gamma_3\left(\frac{Z_m}{c_{44}}\right)\right)J_{m+1}(\xi r)d\xi\right]\right\} \tag{17}$$

$$v(r,\theta,z,t)=-\frac{i}{2}\sum_m\left\{\frac{1}{2\pi i}\int_0^\infty e^{pt}\left[\int_0^\infty \xi\left(-\gamma_1\left(\frac{X_m-Y_m}{2c_{44}}\right)+\gamma_2\left(\frac{X_m+Y_m}{2c_{44}}\right)-\gamma_3\left(\frac{Z_m}{c_{44}}\right)\right)J_{m+1}(\xi r)d\xi-\int_0^\infty \xi\left(\gamma_1\left(\frac{X_m-Y_m}{2c_{44}}\right)+\gamma_2\left(\frac{X_m+Y_m}{2c_{44}}\right)+\gamma_3\left(\frac{Z_m}{c_{44}}\right)\right)J_{m-1}(\xi r)d\xi\right]\right\} \tag{18}$$

$$w(r,\theta,z,t)=\sum_m\left\{\frac{1}{2\pi i}\int e^{pt}\left[\int_0^\infty \xi\left(\Omega_1\left(\frac{X_m-Y_m}{2c_{44}}\right)+\Omega_2\left(\frac{Z_m}{c_{44}}\right)\right)J_m(\xi r)d\xi\right]\right\} \tag{19}$$

where [47]

$$\Omega_1(z,H)=\frac{\vartheta_1\vartheta_2}{2\alpha_3\xi\left(\eta_1\lambda_2^2-\eta_2\lambda_1^2\right)}\mathrm{sgn}(z-H)\left(e^{-\lambda_1|z-H|}-e^{-\lambda_2|z-H|}\right)-\frac{I^+}{I^-}\left[e^{-\lambda_1(z+H)}+e^{-\lambda_2(z+H)}\right]+\frac{2}{I^-}\left[\eta_2\upsilon_2\frac{\vartheta_1}{\vartheta_2}e^{-(\lambda_1 z+\lambda_2 H)}+\eta_1\upsilon_1\frac{\vartheta_2}{\vartheta_1}e^{-(\lambda_2 z+\lambda_1 H)}\right]\Bigg\}. \tag{20}$$

$$\Omega_2(z,H)=\frac{C_{44}}{2\alpha_2C_{33}\left(\lambda_1^2-\lambda_2^2\right)}\left\{\frac{\vartheta_1}{\lambda_1}e^{-\lambda_1|z-H|}-\frac{\vartheta_2}{\lambda_2}e^{-\lambda_2|z-H|}+\frac{I^+}{I^-}\left[\frac{\vartheta_1}{\lambda_1}e^{-\lambda_1(z+H)}+\frac{\vartheta_2}{\lambda_2}e^{-\lambda_2(z+H)}\right]-\frac{2}{I^-}\left[\eta_2\upsilon_2\frac{\vartheta_1}{\lambda_2}e^{-(\lambda_1 z+\lambda_2 H)}+\eta_1\upsilon_1\frac{\vartheta_2}{\lambda_1}e^{-(\lambda_2 z+\lambda_1 H)}\right]\right\} \tag{21}$$

$$\gamma_1(z,H)=\frac{1}{2\left(\eta_1\lambda_2^2-\eta_2\lambda_1^2\right)}\left\{\lambda_1\vartheta_2e^{-\lambda_1|z-H|}-\lambda_2\vartheta_1e^{-\lambda_2|z-H|}-\frac{I^+}{I^-}\left[\lambda_1\vartheta_2e^{-\lambda_1(z+H)}+\lambda_2\vartheta_1e^{-\lambda_2(z+H)}\right]+\frac{2}{I^-}\left[\lambda_1\vartheta_1\eta_2\upsilon_2e^{-(\lambda_1 z+\lambda_2 H)}+\lambda_2\vartheta_2\eta_1\upsilon_1e^{-(\lambda_2 z+\lambda_1 H)}\right]\right\}. \tag{22}$$

$$\gamma_2(z,H)=\frac{1}{2\nu}\left(e^{-\nu|z-H|}+e^{-\nu(z+H)}\right). \tag{23}$$

$$\begin{aligned}\gamma_3(z,H)=\frac{\alpha_3C_{44}\xi}{2\alpha_2C_{33}\left(\lambda_1^2-\lambda_2^2\right)}\Big\{&\operatorname{sgn}(z-H)\left(e^{-\lambda_1|z-H|}-e^{-\lambda_2|z-H|}\right)\\&+\frac{I^+}{I^-}\left[e^{-\lambda_1(z+H)}+e^{-\lambda_2(z+H)}\right]\\&-\frac{2}{I^-}\left[\eta_2\upsilon_2\frac{\lambda_1}{\lambda_2}e^{-(\lambda_1z+\lambda_2H)}+\eta_1\upsilon_1\frac{\lambda_2}{\lambda_1}e^{-(\lambda_2z+\lambda_1H)}\right]\Big\}.\end{aligned} \tag{24}$$

with

$$X_m=\tilde{\tilde{P}}_m^{m-1}-i\tilde{\tilde{Q}}_m^{m-1},\ Y_m=\tilde{\tilde{P}}_m^{m+1}+i\tilde{\tilde{Q}}_m^{m+1},\ Z_m=\tilde{\tilde{R}}_m^{m}$$
$$\eta_k=(\alpha_3-\alpha_2)\lambda_k^2+\xi^2(1+\alpha_1)+\rho_0p^2,\ \vartheta_k=\alpha_3\lambda_k^2-\eta_k$$
$$\upsilon_k=\left(\eta_i-\alpha_3\frac{C_{13}}{C_{33}}\xi^2-\alpha_3\lambda_k^2\right)\lambda_k,\ I^{\pm}=\eta_2\upsilon_1\pm\eta_1\upsilon_2,\ k=1,2,3$$
$$\operatorname{sgn}(z-H)=\begin{cases}+1 & z>H\\-1 & z<H\end{cases} \tag{25}$$

In the same way, one can derive the representations for the stress components, which are eliminated here for brevity see [37,47]. It is emphasized that in Khojasteh et al [47], the results have been presented in the frequency domain, and it is necessary to replace $\omega=-ip$ in Khojasteh et al [47] to derive time domain results, which may be used in this study.

3. Displacement Green's functions

The general solutions of the displacement vector shown in Eqs. (17)–(19) can be specified for the case of concentrated tractions varying with time as Heaviside step function as

$$\mathbf{f}(r,\theta,t)=f_h\frac{\delta(r)}{2\pi r}H(t)\mathbf{e}_h+f_v\frac{\delta(r)}{2\pi r}H(t)\mathbf{e}_z, \tag{26}$$

In Eq. (26), $\delta(.)$ is the Dirac delta function, $H(.)$ is the Heaviside step function, and $\mathbf{e}_h$ is the unit vector in any horizontal direction given by (see also Fig. 2)

$$\mathbf{e}_h=\cos(\theta-\theta_0)\mathbf{e}_r-\sin(\theta-\theta_0)\mathbf{e}_\theta. \tag{27}$$

with $\mathbf{e}_r, \mathbf{e}_\theta$ and $\mathbf{e}_z$ being the unit vectors in radial, angular and vertical directions, respectively. Moreover, f_h and f_v are the magnitudes of point load, which may be used for determination of the transformed loading coefficients X_m, Y_m, Z_m (see Eq. (25)) as:

$$X_m=\begin{cases}e^{-i\theta_0}\frac{f_h}{2\pi p}, & m=1\\0, & m\neq1\end{cases}$$
$$Y_m=\begin{cases}e^{i\theta_0}\frac{f_h}{2\pi p}, & m=-1\\0, & m\neq-1\end{cases},$$
$$Z_m=\begin{cases}\frac{f_v}{2\pi p}, & m=0\\0, & m\neq0\end{cases} \tag{28}$$

Substituting these relations into (17)–(19) results in the displacement components as

$$\begin{aligned}u(r,\theta,z,t)=-\frac{1}{4\pi C_{44}}\Big\{\frac{1}{2\pi i}\int_{\sigma_0+i\infty}^{\sigma_0+i\infty}\frac{e^{pt}}{p}\Big[&2f_v\int_0^\infty\gamma_3\xi J_1(\xi r)d\xi\\&-f_h\cos(\theta-\theta_0)\left(\int_0^\infty(\gamma_1+\gamma_2)\xi J_0(\xi r)d\xi\right.\\&\left.-\int_0^\infty(\gamma_1-\gamma_2)\xi J_2(\xi r)d\xi\right)\Big]dp\Big\}.\end{aligned} \tag{29}$$

$$\begin{aligned}v(r,\theta,z,t)=-\frac{1}{4\pi C_{44}}\Big\{\frac{f_h\cos(\theta-\theta_0)}{2\pi i}\int_{\sigma_0+i\infty}^{\sigma_0+i\infty}\frac{e^{pt}}{p}\Big[\Big(&\int_0^\infty(\gamma_1\\&+\gamma_2)\xi J_0(\xi r)d\xi+\int_0^\infty(\gamma_1-\gamma_2)\xi J_2(\xi r)d\xi\Big)\Big]dp\Big\}.\end{aligned} \tag{30}$$

$$\begin{aligned}w(r,\theta,z,t)=\frac{1}{4\pi C_{44}}\Big\{\frac{1}{2\pi i}\int_{\sigma_0+i\infty}^{\sigma_0+i\infty}\frac{e^{pt}}{p}\Big[&f_v\int_0^\infty\Omega_2\xi J_0(\xi r)d\xi\\&+f_h\cos(\theta-\theta_0)\int_0^\infty\Omega_1\xi J_1(\xi r)d\xi\Big]dp\}\end{aligned} \tag{31}$$

To derive the displacement Green's functions at the free surface of the half-space, the integrals in Eqs. (29)–(31) must be evaluated for $z=0$. At first, by setting $z=0$ in Eqs. (20)–(24), we have

$$\gamma_1(z=0,H)=\frac{\lambda_2\upsilon_1-\lambda_1\upsilon_2}{\left(\eta_1\lambda_2^2-\eta_2\lambda_1^2\right)I^-}\left\{\theta_2\eta_1e^{-\lambda_1H}-\theta_1\eta_2e^{-\lambda_2H}\right\}.$$
$$pt\gamma_2(z=0,H)=\frac{e^{-\nu H}}{\nu}$$
$$\gamma_3(z=0,H)=\frac{\alpha_3C_{44}\xi(\lambda_1\upsilon_2-\lambda_2\upsilon_1)}{\alpha_2C_{33}I^-\left(\lambda_1^2-\lambda_2^2\right)\lambda_1\lambda_2}\left\{\eta_1\lambda_2e^{-\lambda_1H}-\eta_2\lambda_1e^{-\lambda_2H}\right\}$$
$$\Omega_1(z=0,H)=\frac{1}{\alpha_3\xi\left(\eta_1\lambda_2^2-\eta_2\lambda_1^2\right)}\left\{\frac{\vartheta_2\eta_1-\vartheta_1\eta_2}{I^-}\left(\upsilon_1\vartheta_2e^{-\lambda_1H}-\upsilon_2\vartheta_1e^{-\lambda_2H}\right)\right\}.$$
$$\Omega_2(z=0,H)=\frac{C_{44}}{\alpha_2C_{33}\left(\lambda_1^2-\lambda_2^2\right)\lambda_1\lambda_2}\left\{\frac{\eta_2\vartheta_1-\eta_1\theta_2}{I^-}\left(\upsilon_1\lambda_2e^{-\lambda_1H}-\upsilon_2\lambda_1e^{-\lambda_2H}\right)\right\} \tag{32}$$

To facilitate the inversion of the double transform in Eqs. (29)–(31), we use the following change of variable introduced by Cagniard (see [20,37]) in the Hankel inversion integral

$$\xi=px,\quad d\xi=pdx \tag{33}$$

which results in

$$\begin{aligned}u(r,\theta,0,t)=-\frac{1}{4\pi C_{44}}\Big\{\frac{1}{2\pi i}\int_{\sigma_0+i\infty}^{\sigma_0+i\infty}e^{pt}\Big[&2f_v\int_0^\infty\hat{\gamma}_3xJ_1(pxr)dx\\&-f_h\cos(\theta-\theta_0)\left(\int_0^\infty(\hat{\gamma}_1+\hat{\gamma}_2)xJ_0(pxr)dx\right.\\&\left.-\int_0^\infty(\hat{\gamma}_1-\hat{\gamma}_2)xJ_2(pxr)dx\right)\Big]dp\Big\}\end{aligned}$$
$$\begin{aligned}v(r,\theta,0,t)=-\frac{1}{4\pi C_{44}}\Big\{\frac{f_h\cos(\theta-\theta_0)}{2\pi i}\int_{\sigma_0+i\infty}^{\sigma_0+i\infty}e^{pt}\Big[\Big(&\int_0^\infty(\hat{\gamma}_1\\&+\hat{\gamma}_2)xJ_0(pxr)dx+\int_0^\infty(\hat{\gamma}_1-\hat{\gamma}_2)xJ_2(pxr)dx\Big)\Big]dp\Big\}\end{aligned}$$
$$\begin{aligned}w(r,\theta,0,t)=-\frac{1}{4\pi C_{44}}\Big\{\frac{1}{2\pi i}\int_{\sigma_0+i\infty}^{\sigma_0+i\infty}e^{pt}\Big[&f_v\int_0^\infty\hat{\Omega}_2xJ_0(pxr)dx\\&+f_h\cos(\theta-\theta_0)\int_0^\infty\hat{\Omega}_1xJ_1(pxr)dx\Big]dp\Big\}\end{aligned} \tag{34}$$

where

$$\hat{\gamma}_1(z=0,H)=\frac{\hat{\lambda}_2\hat{\upsilon}_1-\hat{\lambda}_1\hat{\upsilon}_2}{\left(\hat{\eta}_1\hat{\lambda}_2^2-\hat{\eta}_2\hat{\lambda}_1^2\right)\hat{I}^-}\left\{\hat{\vartheta}_2\hat{\eta}_1e^{-\hat{\lambda}_1Hp}-\hat{\theta}_1\hat{\eta}_2e^{-\hat{\lambda}_2Hp}\right\}.$$
$$\hat{\gamma}_2(z=0,H)=\frac{e^{-\hat{\nu}Hp}}{\hat{\nu}}$$
$$\hat{\gamma}_3(z=0,H)=\frac{\alpha_3C_{44}x\left(\hat{\lambda}_1\hat{\upsilon}_2-\hat{\lambda}_2\hat{\upsilon}_1\right)}{\alpha_2C_{33}\hat{I}^-}\left(\hat{\lambda}_1^2-\hat{\lambda}_2^2\right)\hat{\lambda}_1\hat{\lambda}_2\left\{\hat{\eta}_1\hat{\lambda}_2e^{-\hat{\lambda}_1Hp}-\hat{\eta}_2\hat{\lambda}_1e^{-\hat{\lambda}_2Hp}\right\}$$
$$\hat{\Omega}_1(z=0,H)=\frac{1}{\alpha_3x\left(\hat{\eta}_1\hat{\lambda}_2^2-\hat{\eta}_2\hat{\lambda}_1^2\right)}\left\{\frac{\hat{\vartheta}_2\hat{\eta}_1-\hat{\vartheta}_1\hat{\eta}_2}{\hat{I}^-}\left(\hat{\upsilon}_1\hat{\vartheta}_2e^{-\hat{\lambda}_1Hp}-\hat{\upsilon}_2\hat{\vartheta}_1e^{-\hat{\lambda}_2Hp}\right)\right\}.$$

$$\hat{\Omega}_2(z=0,H)=\frac{C_{44}}{\alpha_2 C_{33}\left(\hat{\lambda}_1^2-\hat{\lambda}_2^2\right)\hat{\lambda}_1\hat{\lambda}_2}\left\{\frac{\hat{\eta}_2\hat{\vartheta}_1-\hat{\eta}_1\hat{\vartheta}_2}{\hat{I}^-}\left(\hat{\upsilon}_1\hat{\lambda}_2 e^{-\hat{\lambda}_1 Hp}-\hat{\upsilon}_2\hat{\lambda}_1 e^{-\hat{\lambda}_2 Hp}\right)\right\} \tag{35}$$

in which

$$\hat{\lambda}_{1,2}=\sqrt{k_1x^2+k_2\pm\frac{1}{2}\sqrt{k_3x^4+k_4x^2+k_5}}$$
$$\hat{\eta}_k=\left[(\alpha_3-\alpha_2)\hat{\lambda}_k^2+x^2(1+\alpha_1)+\rho_0\right]$$
$$\hat{\vartheta}_k=\left(\alpha_3\hat{\lambda}_k^2-\hat{\eta}_k\right)$$
$$\hat{\upsilon}_k=\left(\hat{\eta}_k-\alpha_3\frac{C_{13}}{C_{33}}x^2-\alpha_3\hat{\lambda}_k^2\right)\hat{\lambda}_k\ \nu=\frac{1}{\sqrt{\alpha_2}}\sqrt{x^2+\rho_0}$$
$$\hat{I}^{\pm}=\hat{\eta}_2\hat{\upsilon}_1\pm\hat{\eta}_1\hat{\upsilon}_2,\ k=1,2,3 \tag{36}$$

It should be noticed that in this case the Laplace transform parameter appears only at the exponential functions and the argument of Bessel functions.

3.1. The case of horizontal surface source

It is emphasized that the case of *vertical surface point force* which results in axisymmetric case, has been treated in Eskandari-Ghadi and Sattar [37] and therefore we discard it in this study. Thus, let us first consider the case of *horizontal surface point force* in which we have $f_v=H=0$ and as a result of this substitution one may write:

$$\hat{\gamma}_1(z=0,H=0)=\frac{\left(\hat{\lambda}_2\hat{\upsilon}_1-\hat{\lambda}_1\hat{\upsilon}_2\right)\left(\hat{\vartheta}_2\hat{\eta}_1-\hat{\vartheta}_1\hat{\eta}_2\right)}{\left(\hat{\eta}_1\hat{\lambda}_2^2-\hat{\eta}_2\hat{\lambda}_1^2\right)\hat{I}^-}.$$
$$\hat{\gamma}_2(z=0,H=0)=\frac{1}{\hat{\nu}}$$
$$\hat{\gamma}_3(z=0,H=0)=\frac{\alpha_3C_{44}x\left(\hat{\lambda}_1\hat{\upsilon}_2-\hat{\lambda}_2\hat{\upsilon}_1\right)\left(\hat{\eta}_1\hat{\lambda}_2-\hat{\eta}_2\hat{\lambda}_1\right)}{\alpha_2C_{33}\hat{I}^-\left(\hat{\lambda}_1^2-\hat{\lambda}_2^2\right)\hat{\lambda}_1\hat{\lambda}_2}$$
$$\hat{\Omega}_1(z=0,H=0)=\frac{\left(\hat{\vartheta}_2\hat{\eta}_1-\hat{\vartheta}_1\hat{\eta}_2\right)\left(\hat{\upsilon}_1\hat{\vartheta}_2-\hat{\upsilon}_2\hat{\vartheta}_1\right)}{\alpha_3x\left(\hat{\eta}_1\hat{\lambda}_2^2-\hat{\eta}_2\hat{\lambda}_1^2\right)\hat{I}^-}.$$
$$\hat{\Omega}_2(z=0,H=0)=\frac{C_{44}\left(\hat{\eta}_2\hat{\vartheta}_1-\hat{\eta}_1\hat{\vartheta}_2\right)\left(\hat{\upsilon}_1\hat{\lambda}_2-\hat{\upsilon}_2\hat{\lambda}_1\right)}{\alpha_2C_{33}\hat{I}^-\left(\hat{\lambda}_1^2-\hat{\lambda}_2^2\right)\hat{\lambda}_1\hat{\lambda}_2}. \tag{37}$$

Now, with the use of the following two identities of Bessel functions

$$J_1(z)=-\frac{dJ_0(z)}{dz}$$
$$J_2(z)=-\left(J_0(z)+\frac{2}{z}\frac{dJ_0(z)}{dz}\right) \tag{38}$$

one may write

$$J_1(pxr)=-\frac{1}{px}\frac{\partial J_0(pxr)}{\partial r}$$
$$J_2(pxr)=-\left(J_0(pxr)+\frac{2}{p^2x^2r}\frac{\partial J_0(pxr)}{\partial r}\right) \tag{39}$$

Eq. (39) shows that to derive the inversion of the integral in Eq. (34) (with $f_v=0$), it is sufficient to compute, only the inverse for the case of the integral involving Bessel function of zero order. The other cases could be derived by the simple identities of Laplace transform as would be seen at the sequel (see Appendix A). Here, we introduce the inverse Laplace transform of functions $T^L(p)$ in the form of

$$T^L(p)=\int_0^\infty xf(x)J_0(prx)dx. \tag{40}$$

in which $f(x)$ is an arbitrary function of x, which approaches zero as $x\to\infty$. The inverse of this function could be determined with the use of the method of Cagniard as (see Appendix A, Eqs. (A2)–(A7)):

$$T(t)=-\frac{2}{\pi}\mathrm{Im}\int_0^{\frac{t}{r}}\frac{\mu f(i\mu)}{\sqrt{t^2-\mu^2r^2}}d\mu \tag{41}$$

For the integrals involving Bessel function of the second order, we have:

$$S^L(p)=\int_0^\infty xf(x)J_2(prx)dx \tag{42}$$

By considering Eq. (39), one may write (see Appendix A, Eq. (A8)–(A12)):

$$S(t)=\frac{2}{\pi}\mathrm{Im}\int_0^{\frac{t}{r}}\frac{\mu f(i\mu)}{\sqrt{t^2-\mu^2r^2}}d\mu+\frac{4}{\pi r^2}\mathrm{Im}\int_0^{\frac{t}{r}}\frac{f(i\mu)}{\mu}\sqrt{t^2-\mu^2r^2}d\mu \tag{43}$$

Finally, for the integrals containing Bessel function of the first order we have

$$N^L(p)=\int_0^\infty xf(x)J_1(prx)dx \tag{44}$$

In this case, the inversion is (see Appendix A, Eqs. (A13) and (A14))

$$N(t)=\frac{2}{\pi}\frac{t}{r}\mathrm{Re}\int_0^{\frac{t}{r}}\frac{f(i\mu)}{\sqrt{t^2-\mu^2r^2}}d\mu \tag{45}$$

Eqs. (41), (43) and (45) could be used to determine the displacement Green's functions at the free surface of the half-space due to surface horizontal point force. The only thing that is left is to notice to the proper representations given in (41), (43) and (45) according to Eq. (34) (for $f_v=0$), with kernels given in Eq. (37). The function $f(x)$ in the above equations must be replaced by corresponding kernel functions in Eq. (37).

3.2. The case of buried source

Now, we consider the case of buried source, namely $H\neq0$, for both horizontal and vertical point force. In this case, by refereeing to Eqs. (34) and (35), and the identities of Bessel functions, we need to find the Laplace inverse transforms of the following two integral equations:

$$K(p)=\int_0^\infty xf(x)e^{-\lambda_iHp}J_0(prx)dx,\quad i=1,2 \tag{46}$$

$$L(p)=\int_0^\infty xf(x)e^{-\nu Hp}J_0(prx)dx, \tag{47}$$

In the first place, we consider Eq. (47), which is corresponding to the $SH-$wave. This wave arises only for the case of horizontal point force and its characteristics contain in the kernel function γ_2. After some complicated but straight forward algebraic manipulations one may obtain the inverse Laplace transform of the functions $L(p)$ as (See Appendix B, Eqs. (B3)–(B36)):

$$L(t)=0,\qquad \zeta<h$$
$$L(t)=\frac{2}{\pi Z}\mathrm{Im}\int_0^{im_1(t)}\frac{xf(x)}{\sqrt{A(x;\ t)}}dx,\qquad h<\zeta<1$$
$$L(t)=\frac{2}{\pi Z}\mathrm{Im}\int_0^{x_\zeta(t)}\frac{xf(x)}{\sqrt{A(x;\ t)}}dx,\qquad \zeta>1 \tag{48}$$

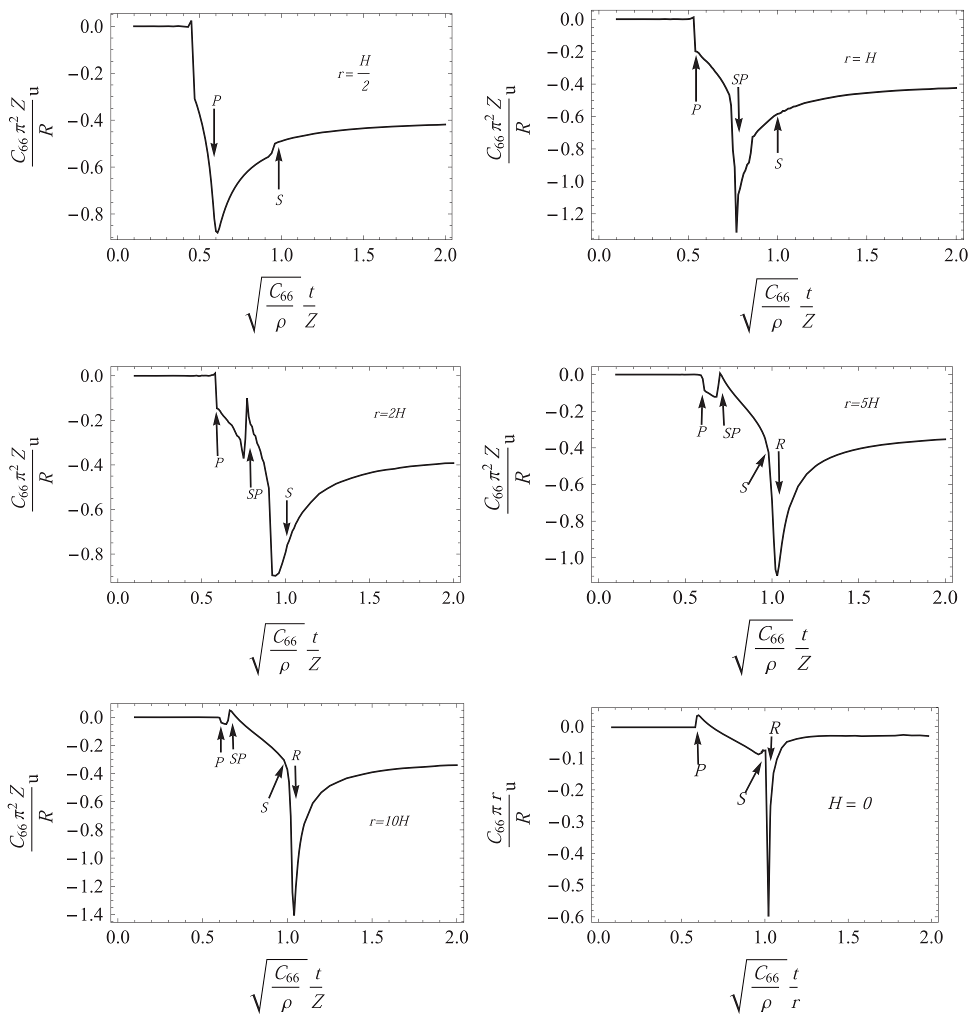

Fig. 3. Surface radial displacement due to buried vertical point force at different epicenteral distance.

where

$$\zeta(t)=\tfrac{t}{aR},\qquad h=\tfrac{H}{\sqrt{\alpha_2}Z},\qquad Z=\sqrt{r^2+\tfrac{H^2}{\alpha_2}}$$

$$m_1(t)=a\zeta\sqrt{1-h^2}-ah\sqrt{1-\zeta^2(t)},$$

$$x_\zeta=ah\sqrt{\zeta^2(t)-1}+ia\zeta(t)\sqrt{1-h^2}$$

$$A(x;\ t)=x^2+a^2(h^2+\zeta^2(t))-2ah\zeta(t)\sqrt{a^2+x^2},\tag{49}$$

The inverse for the Bessel function of the first order, namely

$$Y(p)=\int_0^\infty xf(x)e^{-\nu Hp}J_1(prx)dx,\tag{50}$$

is (see Appendix B, Eqs. (B37)–(B45))

$$Y(t)=0,\qquad \zeta<h$$

$$Y(t)=\frac{2}{\pi r}\mathrm{Im}\int_0^{im_1(t)}\frac{\left(a\zeta-h\sqrt{a^2+x^2}\right)f(x)}{\sqrt{A(x;\ t)}}dx,\qquad h<\zeta<1$$

$$Y(t)=\frac{2}{\pi r}\mathrm{Im}\int_0^{x_\zeta(t)}\frac{\left(a\zeta-h\sqrt{a^2+x^2}\right)f(x)}{\sqrt{A(x;\ t)}}dx,\qquad \zeta>1\tag{51}$$

Finally, For the Bessel function of the second order, we have,

$$D(p)=\int_0^\infty xf(x)e^{-\nu Hp}J_2(prx)dx,\tag{52}$$

while its inverse may be expressed as (see Appendix B, Eqs. (B46)–(B53)):

$$D(t)=0,\qquad \zeta<h$$

$$D(t)=\frac{2}{\pi Z}\mathrm{Im}\int_0^{im_1(t)}f(x)\frac{(1-h^2)x^2+2\left(a\zeta-h\sqrt{a^2+x^2}\right)^2}{x\sqrt{A(x;\ t)}}dx\qquad h<\zeta<1$$

$$D(t)=\frac{2}{\pi Z}\mathrm{Im}\int_0^{x_\zeta}f(x)\frac{(1-h^2)x^2+2\left(a\zeta-h\sqrt{a^2+x^2}\right)^2}{x\sqrt{A(x;\ t)}}dx\qquad \zeta>1\tag{53}$$

Now, we consider the case of $P-$ and $SV-$waves which are corresponding to Eq. (46). In these cases as could be seen in Eq. (36), $\hat{\lambda}_i(i=1,2)$ are complicated functions of x, which does not permit the analytical solution of Eq. (46) to be determined, with the use of a suitable path of integration in general. However for a particular transversely isotropic material, specified by the value of its elastic module, the analytical solution still could be established. Referring to Eq. (36), one could write

$$\hat{\lambda}_i=\sqrt{z_1\pm\frac{1}{2}\sqrt{z_2}}\ ,\quad z_1=k_1x^2+k_2,\quad z_2=k_3x^4+k_4x^2+k_5\tag{54}$$

where z_1 and z_2 would be two complex polynomial functions of $x=\sigma+i\mu$. In the cases where the function z_2 could be written as a perfect square, the inner radical in Eq. (54) is eliminated and we can find the analytical solution with the same procedure explained

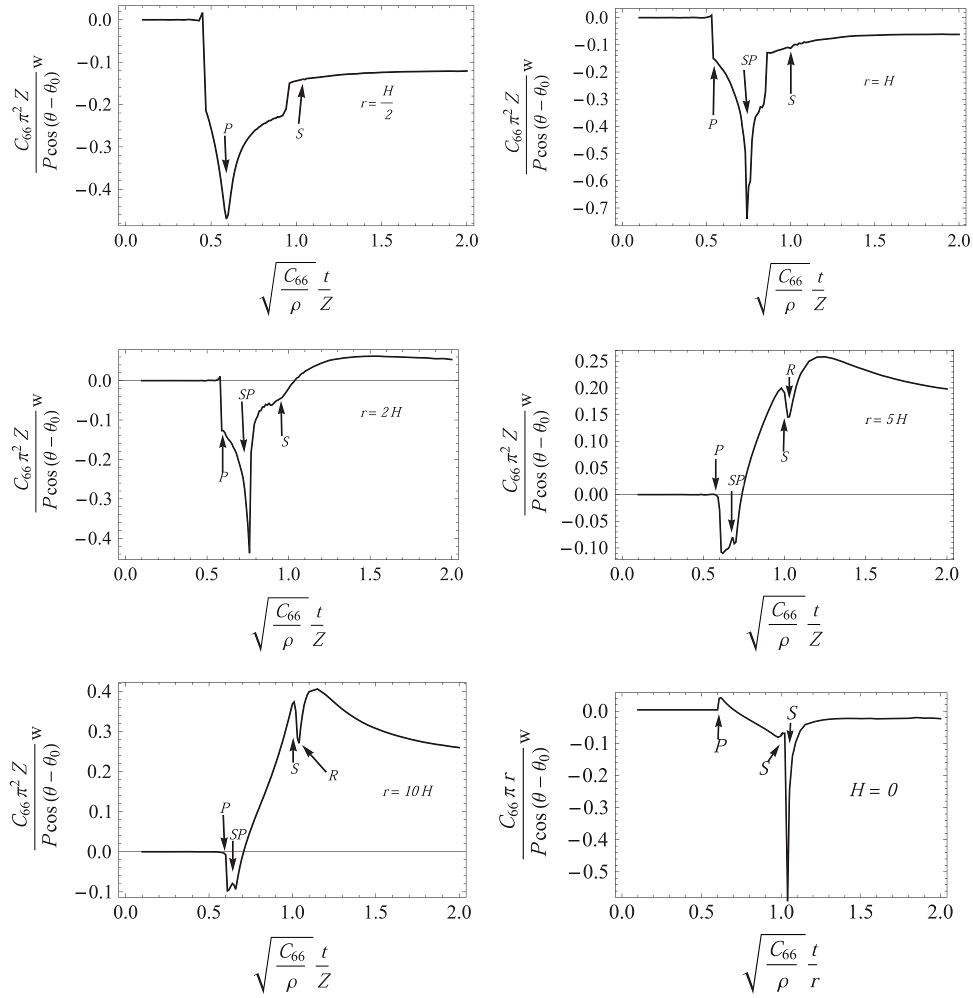

Fig. 4. Surface vertical displacement due to buried horizontal point force at different epicenteral distance.

in the part of $SH-$wave. The polynomial z_2 may be written as a complete square if its discriminate is zero namely

$$\overline{\Delta}=k_4^2-4k_3k_5=0 \tag{55}$$

Due to characteristics of s_1^2 and s_2^2 (see Eq. (10)), The coefficients k_1–k_5 in Eq. (54) are all real and k_2 and k_5 are also positive, (see also Eq. (14)), thus the necessary condition for Eq. (55) to be hold is that

$$k_3>0 \tag{56}$$

From Eqs. (14) and (10), it is seen that $k_3<0$, only if s_1^2 and s_2^2 be complex conjugate. In other words k_3 would be positive if

$$\begin{aligned}
&C_{13}>\sqrt{C_{11}C_{33}} \quad or\\
&C_{13}<-\sqrt{C_{11}C_{33}}-2C_{44} \quad or\\
&\sqrt{C_{11}C_{33}}-2C_{44}<C_{13}<-\sqrt{C_{11}C_{33}}, \qquad with \quad C_{44}^2>C_{11}C_{33} \quad or\\
&-\sqrt{C_{11}C_{33}}<C_{13}<\sqrt{C_{11}C_{33}}-2C_{44}, \qquad with \quad C_{44}^2<C_{11}C_{33}
\end{aligned} \tag{57}$$

and $\overline{\Delta}=0$ if

$$\begin{aligned}
&C_{13}=\sqrt{(C_{44}-C_{11})(C_{44}-C_{33})}-C_{44} \quad or \quad C_{13}=-C_{44} \quad or\\
&C_{13}=-\sqrt{(C_{44}-C_{11})(C_{44}-C_{33})}-C_{44}
\end{aligned} \tag{58}$$

Since the elastic module must be real, it is necessary that in Eq. (58)

$$C_{44}>\max(C_{11},C_{33}) \quad or \quad C_{44}<\min(C_{11},C_{33}) \tag{59}$$

Considering Eqs. (57)–(59), the necessary and sufficient condition for $\overline{\Delta}$ to be zero would be Eq. (58) constrained with

$$C_{44}<\min(C_{11},C_{33}) \tag{60}$$

In this case, one may easily deduce that

$$\hat{\lambda}_{1,2}=\sqrt{\left(k_1\pm\frac{\sqrt{k_3}}{2}\right)x^2+k_2\pm\frac{k_4}{4\sqrt{k_3}}}. \tag{61}$$

Writing

$$\hat{\lambda}_{1,2}=\sqrt{A_\pm}\sqrt{x^2+a^2} \tag{62}$$

with

$$A_\pm=k_1\pm\frac{\sqrt{k_3}}{2}, \qquad a^2=\frac{k_2\pm\frac{k_4}{4\sqrt{k_3}}}{k_1\pm\frac{\sqrt{k_3}}{2}} \tag{63}$$

and considering Eq. (14), it is clear that $A_\pm$ are always positive, since,

$$\begin{aligned}
&A_+=k_1+\frac{\sqrt{k_3}}{2}=s_2^2\\
&A_-=k_1-\frac{\sqrt{k_3}}{2}=s_1^2
\end{aligned} \tag{64}$$

Moreover, k_3 must be positive in the case of $\overline{\Delta}=0$ (see Eq. (56)). Thus, s_2^2 and s_1^2 are real and when they are real, they are also positive. Considering the necessary and sufficient conditions for $\overline{\Delta}=0$, it could be easily proved that a^2 in Eq. (63) is also positive.

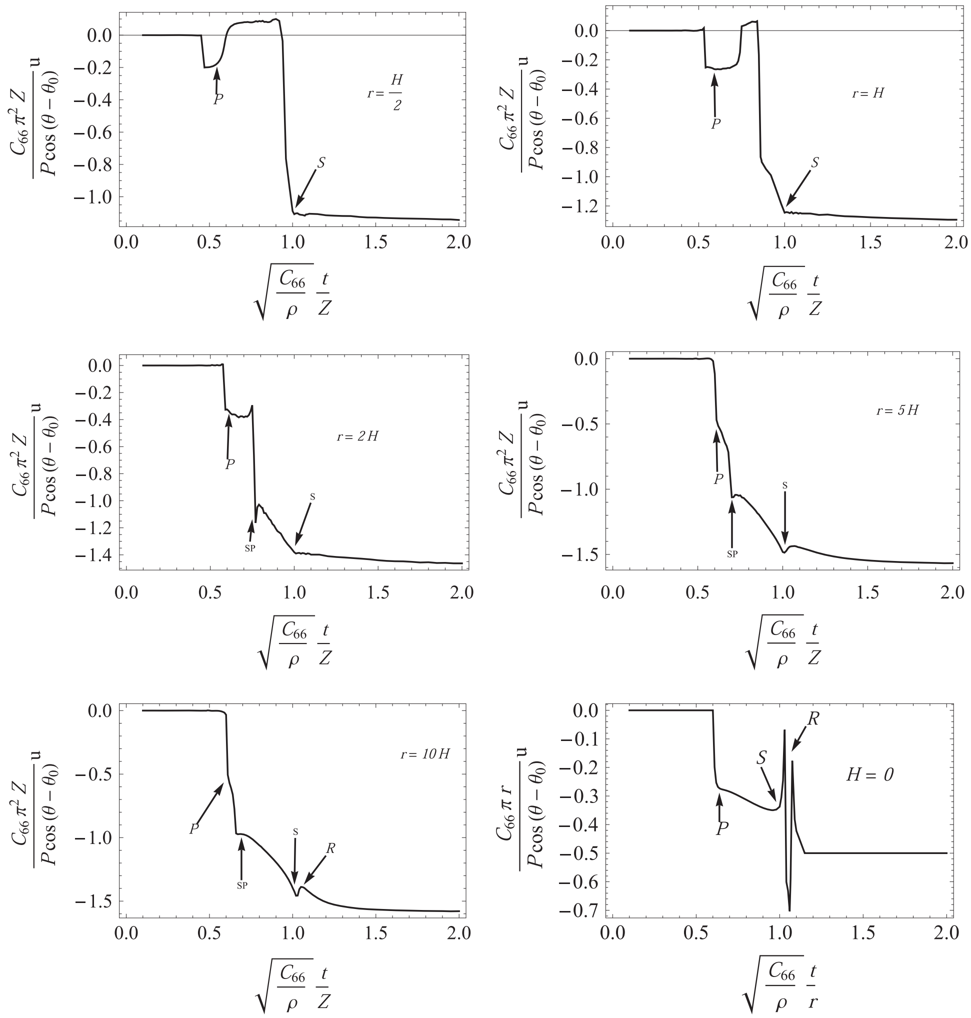

Fig. 5. Surface radial displacement due to buried horizontal point force at different epicenteral distance.

Thus, one may use the results of $SH-$wave motion by the following substitutions

$$\alpha_2 = \frac{1}{A_{\pm}} \tag{65}$$

In the general case of transversely isotropic material, the analytical result could not be obtained and therefore we use the numerical methods for inversion of Laplace and Hankel integral transform.

4. Graphical representation

In the previous section, we have derived the analytical responses of a transversely isotropic half-space, to both buried and surface impulses. In a particular cases, the displacement components have been presented in the form of double integrals related to joint Hankel–Laplace inversion theorem (see Eqs. (29)–(31)). In the general case, the response functions contain different wave fronts including, $P-$, $SV-$, $SH-$ and Rayleigh wave amplitudes and their characteristics lurk on the kernel functions $\gamma_1, \ldots, \Omega_2$ (see Eqs. (20)–(24)). Generally, in a transversely isotropic material, only, For the $SH-$wave, the closed from solution in terms of the integrals with finite limit may be obtained for both buried and surface sources. For other wave fronts, as the authors have tried, the closed form solution could be obtained only for the case of surface source and therefore the full wave motion in the case of buried source needs the application of numerical algorithms for inversion of joint Laplace–Hankel integral transforms. It is emphasized that in isotropic materials as well as a particular class of transversely isotropic material introduced in Eq. (58), the closed from solution could be derived for both surface and buried source and for any wave type. Besides these two special cases, the full wave motion in transversely isotropic materials due to buried source needs the application of suitable numerical method. Recently Raoofian et al [48], introduced an efficient algorithm for inversion of joint Laplace–Hankel integral transforms based on the application of fixed Talbot for Laplace inversion and extrapolating strategy for Hankel inversion. The precision and performance of this algorithm has been tested on similar functions related to wave propagation, where a very good accuracy and reliability can be seen (see [49,50]). For the numerical evaluation, we select a synthetic transversely isotropic material whose mechanical properties in SI unit are $C_{11} = 55,000$, $C_{33} = 159,000$, $C_{44} = 20,000$, $C_{13} = 18,000$, $C_{12} = 15,000$, $\rho = 50$. Here, we emphasized that to investigate the complete behavior of response functions due to buried and surface source in transversely isotropic half-space, it is necessary to derive the response functions for all classes of transversely isotropic material categorized by the sign and interrelation of their elastic module [51,31]. And the result of this paper could be considered as one of those classes.

For the evaluation of the integrals for the surface source, where the analytical solution in terms of integrals with finite limit, may be used, one may very cautious about their integrand functions

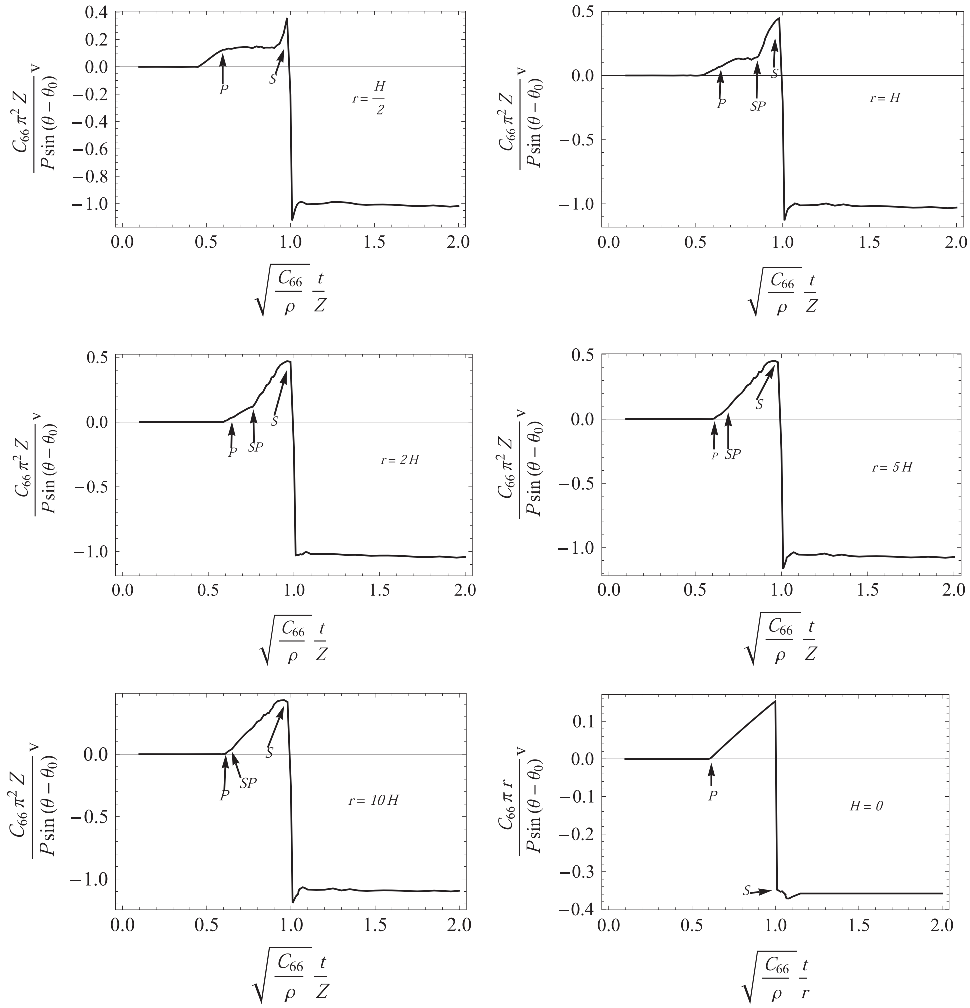

Fig. 6. Surface angular displacement due to buried horizontal point force at different epicenteral distance.

which are not very smooth and well behaved. One must consider the location of the branch points and Rayleigh pole on the path of integration. The Rayleigh pole is the zero of the function $\hat{I}^{-}(x)$ in Eq. (36) which could be numerically found. For the synthetic material used here the pole is located at $x = 0.05177$. The most problematic task was the inversion of radial displacement due to vertical point load and vertical displacement due to horizontal point load and its complexity relates to the arrival of Rayleigh wave. It is emphasized that for the time after the passage of Rayleigh wave, it is necessary that the Cauchy principal value of each integrals are computed.

For numerical computations and graphical representations, we use the Mathematica software Ver. 8. Figs. 3 and 4 show respectively the time histories of vertical and radial displacement at the free surface of a half-space due to application of normal point load varying with time as a Heaviside step function for different radial distance. Also, Figs. 5–7 illustrate, respectively the behavior of vertical, Radial and angular displacements at the free surface of a half-space due to application of horizontal point force varying with time as a Heaviside step function for different radial distance. In these figures and also in the other similar illustrations, P, S, and R denote the arrival time of dilatational, shear, and Rayleigh waves, respectively, and SP is attributed to arrival of diffracted wave, which starts as $S-$wave and is converted into a $P-$wave [20]. It is emphasized that all results presented here are dimensionless, where we use the normalized displacements $(\pi^2 C_{66} Z/R)(u, w)$ for vertical point force and $(\pi^2 C_{66} Z/P\,\cos(\theta-\theta_0))(u,\ \cot(\theta-\theta_0)v, w)$ for horizontal point force. In both cases the normalized time is $\tau = \sqrt{C_{66}/\rho}(t/Z)$.

The above figures show that for small radial distance, the $SP-$wave does not appear and only the amplitudes of $P-$ and $S-$waves are seen. The first arrival of $SP-$wave occurs at $r = H/\sqrt{2}$ which happen before the $S-$wave. The Rayleigh wave arrives only at large epicentral distances from the source particularly its first arrival is seen at $r = 5H$. When the applied loads is vertical, after the arrival of Rayleigh wave, the vertical displacement immediately becomes constant, which is corresponding to its steady state manner. On the other hand, the radial displacement tends to its steady state manner in a monotone fashion. However, when the applied load is horizontal this situation becomes reverse. The Rayleigh wave have no amplitude in the angular displacement which is a proof of the elliptical motion of a material point in planes normal to $\mathbf{e}_\theta$. When the depth of the source tends to zero or as $r/H \to \infty$, the $SP-$wave reaches to the $P-$wave and they become coalescent. In this case, the amplitude of Rayleigh wave tends to infinity and the wave front becomes discontinuous at the arrival time of Rayleigh wave.

Since the vertical normal stress is interested to geotechnical engineers, we also present the behavior of normal stress due to application of vertical point load. In Fig. 7, we illustrate the variations of normal stress as a function of radial distance (upper figures), depth (middle figures), and time respectively (lower figures). As could be seen, the normal stress has an oscillatory behavior with a radial distance and tends to zero with an

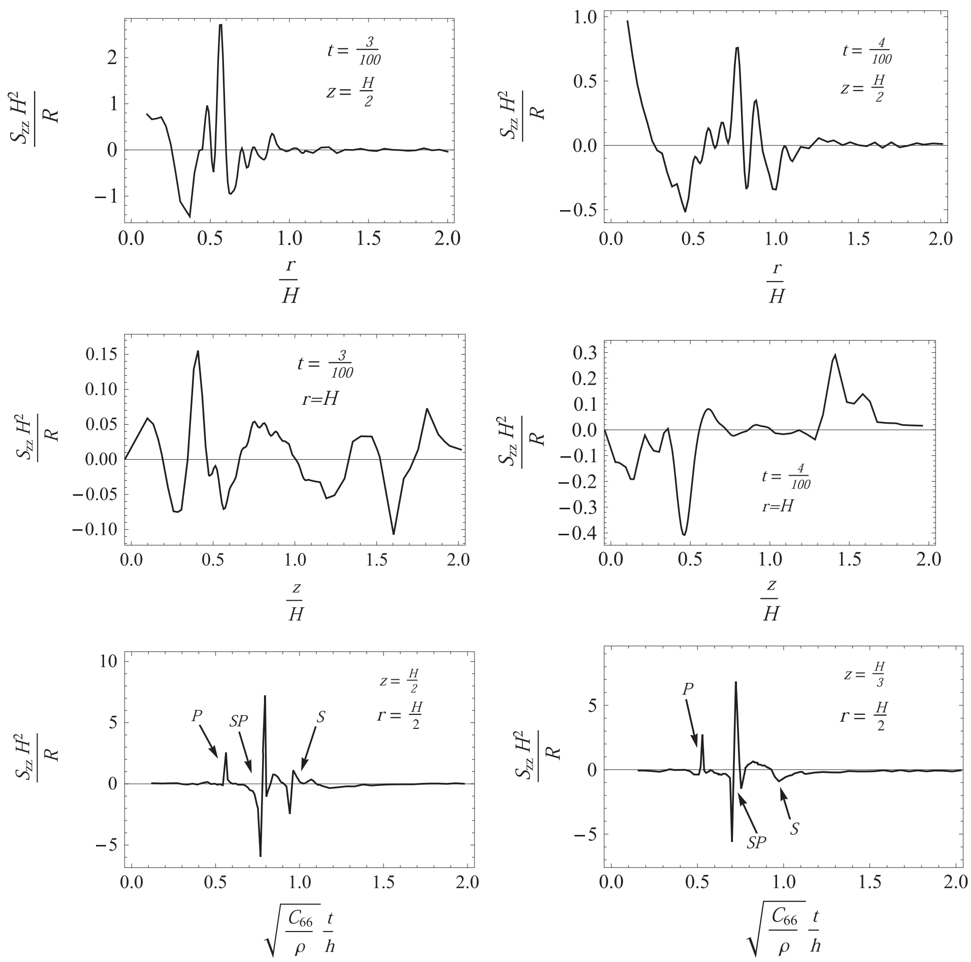

Fig. 7. Behavior of normal stress in a terms of radial distance, depth and time.

oscillatory manner. Due to boundary conditions of the problem, the normal stress is zero at the free surface as it is evident from figure. The time histories of normal stress marks the arrival time of different wave front including $P-$, $SP-$ and Rayleigh wave. Moreover after the passage of S wave the stress becomes zero.

5. Conclusion

The asymmetric transient responses of a transversely isotropic half-space under an arbitrary time-dependent surface and buried tractions have been derived. The general solutions have been investigated for special loading functions which varying as Heaviside step function in time, and also numerically evaluated for a synthetic transversely isotropic material. For the case of surface source, the closed form solution has been obtained by the Cagnirad method and represented in terms of integrals with finite limit. For the case of buried source, where the more sophisticated integrand functions are involved, the closed form solution could be obtained, only for a particular transversely isotropic material in terms of the integrals with finite limits. In the process of numerical evaluations, some special attentions are required to be paid for the presence of branch points and pole at the pass of integration. For the general cases, where the closed from solution does not exist, the numerical inversion of joint Hankel–Laplace integral transform is applied based on suitable and efficient algorithms.

The fundamental solutions derived at this study, are applicable as kernels in the boundary element method or boundary integral formulations for the numerical treatment of more complicated elastodynamic problems involving half-space geometries.

Acknowledgments

The partial support from the University of Tehran through 27840/1/07 to M. E.-G. during this work is gratefully acknowledged. In addition, the authors would like to express their sincere gratitude to Mr. Farzam Fatolahzade for his cooperation in the numerical evaluation of this study.

Appendix A. Derivation of the inverse of Laplace transforms for the case of horizontal surface source

By Mehler–Sonin formula one could represent the Bessel function of the zero order by the following integral equation [52]

$$J_0(z) = \frac{2}{\pi}\mathrm{Im}\int_1^\infty \frac{e^{isz}}{\sqrt{s^2-1}}ds \tag{A1}$$

from which Eq. (40) may be written as

$$\begin{aligned} T^L(p) &= \frac{2}{\pi}\mathrm{Im}\int_0^\infty xf(x)dx\int_1^\infty \frac{e^{iprxs}}{\sqrt{s^2-1}}ds \\ &= \frac{2}{\pi}\mathrm{Im}\int_1^\infty \frac{ds}{\sqrt{s^2-1}}\int_0^\infty xf(x)e^{p(irxs)}dx \end{aligned} \tag{A2}$$

Now, in the complex $x=\sigma+i\mu$ plane, we choose a contour for which the coefficients of p in exponential functions in Eq. (A2) be real [20,21]. Therefore, we must find a path of integration from the solution of the following equation

$$\mathrm{Im}[irxs]=0 \quad \Rightarrow \mathrm{Im}\left[ir(\sigma+i\mu)s\right]=0 \tag{A3}$$

It is clear that this path is located on an imaginary axis $x=i\mu$ ($\sigma=0$) and therefore we have

$$T^L(p)=-\frac{2}{\pi}\mathrm{Im}\int_1^\infty \frac{ds}{\sqrt{s^2-1}}\int_0^\infty \mu f(i\mu)e^{-pr\mu s}d\mu \tag{A4}$$

Now, we use the following change of variable in the first integral

$$s=\frac{t}{\mu r},\ ds=\frac{dt}{r\mu} \tag{A5}$$

which results in

$$T^L(p)=-\frac{2}{\pi}\mathrm{Im}\int_{\mu r}^\infty\left[\int_0^\infty \frac{\mu f(i\mu)}{\sqrt{t^2-\mu^2r^2}}d\mu\right]e^{-pt}dt= -\frac{2}{\pi}\mathrm{Im}\int_0^\infty\left[\int_0^\infty \frac{\mu f(i\mu)H(t-\mu r)}{\sqrt{t^2-\mu^2r^2}}d\mu\right]e^{-pt}dt \tag{A6}$$

From Eq. (A6) and the definition of Laplace transform, it is clear that

$$T(t)=-\frac{2}{\pi}\mathrm{Im}\int_0^\infty \frac{\mu f(i\mu)H(t-\mu r)}{\sqrt{t^2-\mu^2r^2}}d\mu=-\frac{2}{\pi}\mathrm{Im}\int_0^{\frac{t}{r}}\frac{\mu f(i\mu)}{\sqrt{t^2-\mu^2r^2}}d\mu \tag{A7}$$

where $T(t)$ is the inverse Laplace transform of $T^L(p)$. For the integrals involving Bessel function of the second order, we have from Eq. (39):

$$S^L(p)=\int_0^\infty xf(x)J_2(prx)dx=\int_0^\infty xf(x)\left[-J_0(pxr)-\frac{2}{p^2x^2r}\frac{\partial J_0(pxr)}{\partial r}\right]dx$$
$$=-\int_0^\infty xf(x)J_0(pxr)dx-\frac{2}{r}\frac{\partial}{\partial r}\int_0^\infty \frac{g(x)}{x}\frac{J_0(pxr)}{p^2}dx=-S_1^L(p)-S_2^L(p) \tag{A8}$$

The solution for the first part of the above integral is the same as Eq. (A7). However, for the second part, after using Mehler–Sonine formula and taking the integration on the imaginary axis $x=i\mu$, we have

$$S_2^L(p)=\frac{4}{\pi r}\mathrm{Im}\frac{\partial}{\partial r}\int_0^\infty\left[\int_0^\infty \frac{f(i\mu)H(t-\mu r)}{\mu p^2\sqrt{t^2-\mu^2r^2}}d\mu\right]e^{-pt}dt \tag{A9}$$

If $\overline{F}(p)$ is the Laplace transform of a function $f(t)$, then [53]:

$$L^{-1}\left\{\frac{\overline{F}(p)}{p}\right\}=\int_0^t f(u)du,\quad L^{-1}\left\{\frac{\overline{F}(p)}{p^2}\right\}=\int_0^t\left[\int_0^\tau f(u)du\right]d\tau. \tag{A10}$$

where L^{-1} is used as the inverse Laplace operator. Using the above identities of Laplace transform, and after some algebraic manipulations, one may write the inverse of $S_2^L(p)$ as

$$S_2(t)=-\frac{4}{\pi r^2}\mathrm{Im}\int_0^{\frac{t}{r}}\frac{f(i\mu)}{\mu}\sqrt{t^2-\mu^2r^2}d\mu \tag{A11}$$

Thus, from Eq. (A8) one may write

$$S(t)=\frac{2}{\pi}\mathrm{Im}\int_0^{\frac{t}{r}}\frac{\mu f(i\mu)}{\sqrt{t^2-\mu^2r^2}}d\mu+\frac{4}{\pi r^2}\mathrm{Im}\int_0^{\frac{t}{r}}\frac{f(i\mu)}{\mu}\sqrt{t^2-\mu^2r^2}d\mu \tag{A12}$$

For the integrals containing Bessel function of the first order we have from Eq. (39)

$$N(p)=\int_0^\infty xf(x)J_1(prx)dx=-\frac{\partial}{\partial r}\int_0^\infty h(x)\frac{J_0(pxr)}{p}dx \tag{A13}$$

In this case by using Eq. (A10) one may obtain

$$N(t)=\frac{2}{\pi}\frac{t}{r}\mathrm{Re}\int_0^{\frac{t}{r}}\frac{f(i\mu)}{\sqrt{t^2-\mu^2r^2}}d\mu \tag{A14}$$

Appendix B Derivation of the inverse Laplace transforms for the case of buried source

Using the Mehler–Sonine representation (Eq. (A1)) in conjunction with the change of variable $s=ch\varphi$, where $ch(.)$ stands for the hyperbolic cosine function, one may write Eqs. (45) and (47) as:

$$K(p)=\frac{2}{\pi}\mathrm{Im}\int_0^\infty d\varphi\int_0^\infty x\,f(x)e^{-p(H\hat{\lambda}_i-irxch\varphi)}dx$$
$$L(p)=\frac{2}{\pi}\mathrm{Im}\int_0^\infty d\varphi\int_0^\infty x\,f(x)e^{-p(H\nu-irxch\varphi)}dx \tag{B1}$$

As we have done in the previous section, we should find a path on the complex $x=\sigma+i\mu$ plane, for which the coefficients of p in the exponential function be a real quantity. In this case, the path of integration is found from the solutions of the following equations

$$\mathrm{Im}\left(H\hat{\lambda}_i-irxch\varphi\right)=0,\quad i=1,2 \tag{B2}$$

$$\mathrm{Im}(H\nu-irxch\varphi)=0 \tag{B3}$$

But contrary to the previous cases of surface source, here this path is no longer collapsed on $x=i\mu$ or on an imaginary axis. We are trying to find the solution of the above equations in the form of $\mu=f(\sigma)$, which define a curve in $\sigma-\mu$ plane, from which the path of integration may be obtained. In the first place, we consider Eq. (B3), which is corresponding to the $SH-$source. Solving this equation results in two contours as

$$\sigma=0 \qquad or \qquad x=i\mu$$
$$\mu=\left(\mu_0^2+\kappa^2ch^2\phi\sigma^2\right)=f(\sigma) \qquad or \qquad x=\sigma+if(\sigma) \tag{B4}$$

with

$$\kappa=\frac{r}{H}\sqrt{\alpha_2},\ \mu_0^2=\frac{a^2\kappa^2ch^2\phi}{1+\kappa^2ch^2\phi},\ a^2=\rho_0 \tag{B5}$$

It is clear that the portion $\sigma=0$ ($x=i\mu$) should be followed only for $0<\mu<\mu_0$, and for the second part, the path of integration is on $x=\sigma+if(\sigma)$ with $f(\sigma)$ given in (B4). Therefore, we have

$$L(p)=\frac{2}{\pi}\mathrm{Im}\int_0^\infty d\phi\int_0^\infty xf(x)e^{-p(H\nu-irxch\varphi)}dx$$
$$=\frac{2}{\pi}\mathrm{Im}\int_0^\infty d\phi\int_0^{\mu_0} xf(x)e^{-p(H\nu-irxch\varphi)}dx$$
$$+\frac{2}{\pi}\mathrm{Im}\int_0^\infty d\phi\int_{\mu_0}^\infty xf(x)e^{-p(H\nu-irxch\varphi)}dx=L_1(p)+L_2(p) \tag{B6}$$

For the first integral (L_1), we must substitute $x=i\mu$ and for the second integral (L_2), we must substitute $x=\sigma+if(\sigma)$ (see Eq. (B4)). Moreover, along the latter path one may write

$$x=\frac{\sqrt{\mu^2-\mu_0^2}}{\kappa ch\phi}+i\mu,\qquad dx=\left(\frac{\mu}{\kappa ch\phi\sqrt{\mu^2-\mu_0^2}}+i\right)d\mu$$
$$H\nu-irxch\varphi=\frac{\mu H}{\sqrt{\alpha_2}}\left(\kappa ch\phi+\frac{1}{\kappa ch\phi}\right). \tag{B7}$$

At first, we consider the integral of L_2 which by the above equations may be expressed as

$$L_2(p)=\frac{2}{\pi}\mathrm{Im}\int_0^\infty d\phi\int_{\mu_0}^\infty\left[\left(\frac{\sqrt{\mu^2-\mu_0^2}}{\kappa ch\phi}+i\mu\right)f\left(\frac{\sqrt{\mu^2-\mu_0^2}}{\kappa ch\phi}+i\mu\right)\times e^{-\frac{pH\mu}{\sqrt{\alpha_2}}\left(\kappa ch\phi+\frac{1}{\kappa ch\phi}\right)}\left(\frac{\mu}{\kappa ch\phi\sqrt{\mu^2-\mu_0^2}}+i\right)\right]d\mu \tag{B8}$$

Now, if we use the following change of variable

$$\mu=\mu_0 y\qquad\begin{cases}\mu=\mu_0 & \Rightarrow\quad y=1\\ \mu=\infty & \Rightarrow\quad y=\infty\end{cases}$$

$$ch\psi=\frac{\sqrt{1+\kappa^2ch^2\phi}}{\sqrt{1+\kappa^2}}\qquad\begin{cases}\phi=0 & \Rightarrow\quad \psi=0\\ \phi=\infty & \Rightarrow\quad \psi=\infty\end{cases} \tag{B9}$$

then we have

$$\kappa ch\phi=\frac{\sqrt{ch^2\psi-h^2}}{h},\qquad d\mu=\mu_0dy,\qquad h=\frac{H}{Z\sqrt{\alpha_2}}$$
$$\mu_0=\frac{a}{ch\psi}\sqrt{ch^2\psi-h^2}=\mu_0(\psi),\qquad d\phi=\frac{a}{\mu_0}d\psi,\qquad Z=\sqrt{r^2+\frac{H^2}{\alpha_2}} \tag{B10}$$

Substituting the above results into Eq. (B8), we have

$$L_2(p)=\frac{2a}{\pi}\mathrm{Im}\int_0^\infty\mu_0(\psi)d\psi\int_1^\infty\left[\left(\frac{h\sqrt{y^2-1}}{\sqrt{ch^2\psi-h^2}}+iy\right)f\times\left(\frac{ah\sqrt{y^2-1}}{ch\psi}+i\mu_0(\psi)y\right)\times e^{-paZych\psi}\left(\frac{hy}{\sqrt{y^2-1}\sqrt{ch^2\psi-h^2}}+i\right)\right]dy \tag{B11}$$

Since the coefficient of p in the above integral is real, we consider the following change of variable

$$t=aZch\psi y\quad:\quad\begin{cases}y=1 & t=aZch\psi\\ y=\infty & t=\infty\end{cases}$$
$$dy=\frac{dt}{aZch\psi} \tag{B12}$$

As a result Eq. (B11) may be written as

$$L_2(p)=\frac{2}{\pi Z}\mathrm{Im}\int_0^\infty\mu_0(\psi)d\psi\int_{aZch\psi}^\infty g(t,\psi)e^{-pt}dt \tag{B13}$$

in which

$$g(t,\psi)=\frac{1}{ch\psi\sqrt{ch^2\psi-h^2}}\left(h\sqrt{y(t)^2-1}+iy(t)\sqrt{ch^2\psi-h^2}\right)\times\left(\frac{hy(t)}{\sqrt{y(t)^2-1}\sqrt{ch^2\psi-h^2}}+i\right)f\left(\frac{ah\sqrt{y(t)^2-1}}{ch\psi}+i\frac{ay(t)\sqrt{ch^2\psi-h^2}}{ch\psi}\right) \tag{B14}$$

where $y(t)=t/aZch\psi$. Changing the order of integration results in

$$L_2(p)=\frac{2}{\pi Z}\mathrm{Im}\int_0^\infty\left[\int_0^{ch^{-1}\zeta}\mu_0(\psi)g(t,\psi)H(t-aZ)d\psi\right]e^{-pt}dt$$
$$\zeta=\frac{t}{aZ} \tag{B15}$$

Using the definition of Laplace transform

$$L_2(t)=0,\quad t<aZ$$
$$L_2(t)=\frac{2}{\pi Z}\mathrm{Im}\int_0^{ch^{-1}\zeta}\mu_0(\psi)g(t,\psi)d\psi,\quad t>aZ \tag{B16}$$

The above integral could be further simplified by using the change of variable $y=\zeta/ch\psi$, which by considering Eqs. (B14)–(B16) results in:

$$L_2(t)=\frac{2a}{\pi Z\zeta}\mathrm{Im}\int_1^\zeta\frac{y}{\sqrt{\zeta^2-y^2}}f[\alpha(y)]\beta(y)dy,\qquad\zeta>1$$
$$\alpha(y)=\frac{ay}{\zeta}\left[h\sqrt{y^2-1}+i\sqrt{\zeta^2-h^2y^2}\right]$$
$$\beta(y)=\left(h\sqrt{y^2-1}+i\sqrt{\zeta^2-h^2y^2}\right)\left(\frac{hy^2}{\sqrt{y^2-1}\sqrt{\zeta^2-h^2y^2}}+i\right) \tag{B17}$$

Considering the change of variable $x=\alpha(y)$ in the above equation one could easily check that

$$dx=\frac{1}{i}\frac{a}{\zeta}\beta(y)dy$$
$$\frac{y}{\sqrt{\zeta^2-y^2}}=-\frac{ix}{\sqrt{x^2+a^2(h^2+\zeta^2)-2ah\zeta\sqrt{a^2+x^2}}} \tag{B18}$$

With the use of the relations (B18) one may write

$$L_2(t)=\frac{2}{\pi Z}\mathrm{Im}\int_{x_1}^{x_\zeta}\frac{xf(x)}{\sqrt{A(x)}},\qquad\zeta>1$$
$$x_1=\alpha(y=1)=\frac{ia}{\zeta}\sqrt{\zeta^2-h^2},\quad x_\zeta=\alpha(y=\zeta)$$
$$=ah\sqrt{\zeta^2-1}+ia\zeta\sqrt{1-h^2} \tag{B19}$$

where

$$A(x)=x^2+a^2(h^2+\zeta^2)-2ah\zeta\sqrt{a^2+x^2} \tag{B20}$$

Now, we consider the integral of $L_1(p)$, which after change of variable $x=i\mu$ is

$$L_1(p)=-\frac{2}{\pi}\mathrm{Im}\int_0^\infty d\phi\int_0^{\mu_0}\mu f(i\mu)e^{-p\left(H\sqrt{\frac{a^2-\mu^2}{\alpha_2}}+r\mu ch\varphi\right)}d\mu \tag{B21}$$

Since for $0<\mu<\mu_0$ the coefficient of p in the exponential function is real, we can write

$$t=\left(H\sqrt{\frac{a^2-\mu^2}{\alpha_2}}+r\mu ch\varphi\right)\quad:\begin{cases}\mu=0, & t=a\frac{H}{\sqrt{\alpha_2}}\\ \mu=\mu_0 & t=aH\sqrt{\frac{1+\kappa^2ch^2\phi}{\alpha_2}}\end{cases} \tag{B22}$$

Moreover, from Eq. (B22) we have

$$\mu(t,\phi)=\frac{1}{1+\kappa^2ch^2\phi}\left[\frac{t\sqrt{\alpha_2}}{H}\kappa ch\phi-\sqrt{a^2(1+\kappa^2ch^2\phi)-\frac{t^2\alpha_2}{H^2}}\right] \tag{B23}$$

Therefore, one may write Eq. (B21) as:

$$L_1(p)=-\frac{2}{\pi}\mathrm{Im}\int_0^\infty d\phi\int_{a\frac{H}{\sqrt{\alpha_2}}}^{a\frac{H}{\sqrt{\alpha_2}}\sqrt{1+\kappa^2ch^2\phi}}h(t,\phi)e^{-pt}dt \tag{B24}$$

in which

$$h(t,\phi)=\mu(t,\phi)f(i\mu(t,\phi))\frac{d\mu(t,\phi)}{dt} \tag{B25}$$

By changing the order of integration we have

$$L_1(p)=-\frac{2}{\pi}\mathrm{Im}\left\{\int_{a\frac{H}{\sqrt{\alpha_2}}}^{aH\sqrt{\frac{1+\kappa^2}{\alpha_2}}}\left[\int_0^\infty g(t,\phi)d\phi\right]e^{-pt}dt\right.$$

$$+\int_{aH\sqrt{(1+\kappa^2)/\alpha_2}}^{\infty}\left[\int_{\varepsilon}^{\infty}g(t,\phi)d\phi\right]e^{-pt}dt\Bigg\}$$

$$\varepsilon = ch^{-1}\left(\frac{1}{h\kappa}\sqrt{\zeta^2-h^2}\right) \tag{B26}$$

Finally, from the above equations and the definition of the Laplace transform we have

$$\begin{aligned} L_1(t)&=0, && t<\frac{aH}{\sqrt{\alpha_2}} \quad or \quad \zeta<h \\ L_1(t)&=-\frac{2}{\pi}\mathrm{Im}\int_0^{\infty}g(t,\phi)d\phi, && \frac{aH}{\sqrt{\alpha_2}}<t<aH\sqrt{\frac{1+\kappa^2}{\alpha_2}} \quad or \quad h<\zeta<1 \\ L_1(t)&=-\frac{2}{\pi}\mathrm{Im}\int_{\varepsilon}^{\infty}g(t,\phi)d\phi, && t>\frac{aH}{c}\sqrt{\frac{1+\kappa^2}{\alpha_2}} \quad or \quad \zeta>1 \end{aligned} \tag{B27}$$

The above integrals could be further simplified by the following change of variable (see Eq. (B25))

$$x=\mu(t,\phi) \quad \Rightarrow \quad d\phi=\frac{d\phi}{d\mu}dx \tag{B28}$$

Therefore we have

$$\begin{aligned} L_1(t)&=0, && \zeta<h \\ L_1(t)&=-\frac{2}{\pi}\mathrm{Im}\int_{m_1}^{m_2}xf(ix)\frac{d\mu}{dt}\frac{d\phi}{d\mu}dx, && h<\zeta<1 \\ L_1(t)&=-\frac{2}{\pi}\mathrm{Im}\int_{n_1}^{n_2}xf(ix)\frac{d\mu}{dt}\frac{d\phi}{d\mu}dx, && \zeta>1 \end{aligned} \tag{B29}$$

Refereeing to Eq. (B22) one may write

$$x=\mu(t,\phi) \quad \Rightarrow \quad \kappa ch\phi=\frac{t\sqrt{\alpha_2}}{Hx}-\frac{\sqrt{a^2-x^2}}{x} \tag{B30}$$

From the above equation we have

$$\begin{aligned} \frac{d\mu}{dt}\frac{d\phi}{d\mu}&=\frac{d\phi}{dt}=-\frac{1}{Z\sqrt{a^2(h^2+\zeta^2)-x^2-2ah\zeta\sqrt{a^2-x^2}}} \\ m_1&=\mu(t,0)=a\left[\zeta\sqrt{1-h^2}-h\sqrt{1-\zeta^2}\right] \\ n_1&=\mu(t,\varepsilon)=\frac{a}{\zeta}\sqrt{\zeta^2-h^2} \\ m_2&=n_2=\mu(t,\infty)=0 \end{aligned} \tag{B31}$$

Finally one may write

$$\begin{aligned} L_1(t)&=0, && \zeta<h \\ L_1(t)&=-\frac{2}{\pi Z}\mathrm{Im}\int_0^{m_1}\frac{xf(ix)}{\sqrt{B(x)}}dx, && h<\zeta<1 \\ L_1(t)&=-\frac{2}{\pi Z}\mathrm{Im}\int_0^{n_1}\frac{xf(ix)}{\sqrt{B(x)}}dx, && \zeta>1 \end{aligned} \tag{B32}$$

where

$$B(x)=a^2(h^2+\zeta^2)-x^2-2ah\zeta\sqrt{a^2-x^2} \tag{B33}$$

From Eqs. (B33) and (B20) it is clear that

$$B(x)=A(ix) \tag{B34}$$

Therefore on may write Eq. (B32) in the form of

$$\begin{aligned} L_1(t)&=0, && \zeta<h \\ L_1(t)&=\frac{2}{\pi Z}\mathrm{Im}\int_0^{im_1}\frac{xf(x)}{\sqrt{A(x)}}dx, && h<\zeta<1 \\ L_1(t)&=\frac{2}{\pi Z}\mathrm{Im}\int_0^{in_1}\frac{xf(x)}{\sqrt{A(x)}}dx, && \zeta>1 \end{aligned} \tag{B35}$$

Considering Eq. (B35) and (B19) and (B6), one may arrive at Eq. (48) as

$$\begin{aligned} L(t)&=0, && \zeta<h \\ L(t)&=\frac{2}{\pi Z}\mathrm{Im}\int_0^{im_1}\frac{xf(x)}{\sqrt{A(x)}}dx, && h<\zeta<1 \\ L(t)&=\frac{2}{\pi Z}\mathrm{Im}\int_0^{x_\zeta}\frac{xf(x)}{\sqrt{A(x)}}dx, && \zeta>1 \end{aligned} \tag{B36}$$

Now we consider the integral involving the Bessel function of the first order, namely

$$Y(p)=\int_0^{\infty}xf(x)e^{-\nu Hp}J_1(prx)dx \tag{B37}$$

By considering the first identity in Eq. (39), and the Mehler–Sonin representation, one may write the above equation as:

$$Y(p)=-\frac{2}{\pi}\mathrm{Re}\int_0^{\infty}ch\varphi\, d\varphi\int_0^{\infty}xf(x)e^{-p(\nu H-irxch\varphi)}dx=Y_1(p)+Y_2(p) \tag{B38}$$

This is similar in the form to Eq. (B1), the only diffidence consisting in the appearance of the extra factor $ch\varphi$. By considering Eq. (B10), this adds the following factor in the integrand of $Y_2(p)$

$$ch\varphi=\frac{\sqrt{ch^2\psi-h^2}}{\kappa h} \tag{B39}$$

Therefore one may write Eq. (B17) (here L_2 should be replaced by Y_2) as

$$Y_2(t)=\frac{2a}{\pi r\zeta}\mathrm{Re}\int_1^{\zeta}\frac{\sqrt{\zeta^2-h^2y^2}}{\sqrt{\zeta^2-y^2}}f[\alpha(y)]\beta(y)dy, \qquad \zeta>1 \tag{B40}$$

As before by considering the change of variable $x=\alpha(y)$ one may write

$$\frac{\sqrt{\zeta^2-h^2y^2}}{\sqrt{\zeta^2-y^2}}=\frac{a\zeta-h\sqrt{a^2+x^2}}{\sqrt{A(x)}} \tag{B41}$$

And finally

$$\begin{aligned} Y_2(t)&=0 && \zeta<1 \\ Y_2(t)&=\frac{2}{\pi r}\mathrm{Im}\int_{x_1}^{x_\zeta}\frac{\left(a\zeta-h\sqrt{a^2+x^2}\right)f(x)}{\sqrt{A(x)}}, && \zeta>1 \end{aligned} \tag{B42}$$

In the same way, according to Eq. (B30), $ch\varphi$ adds the following factor in the the integrand of $Y_1(p)$,

$$ch\varphi=\frac{a\zeta-h\sqrt{a^2-x^2}}{\sqrt{1-h^2}x} \tag{B43}$$

Therefore one may write:

$$\begin{aligned} Y_1(t)&=0, && \zeta<h \\ Y_1(t)&=-\frac{2}{\pi r}\mathrm{Im}\int_0^{m_1}\frac{\left(a\zeta-h\sqrt{a^2-x^2}\right)f(ix)}{\sqrt{B(x)}}dx, && h<\zeta<1 \\ Y_1(t)&=-\frac{2}{\pi r}\mathrm{Im}\int_0^{n_1}\frac{\left(a\zeta-h\sqrt{a^2-x^2}\right)f(ix)}{\sqrt{B(x)}}dx, && \zeta>1 \end{aligned} \tag{B44}$$

And finally we have:

$$\begin{aligned} Y(t)&=0, && \zeta<h \\ Y(t)&=\frac{2}{\pi r}\mathrm{Im}\int_0^{im_1}\frac{\left(a\zeta-h\sqrt{a^2+x^2}\right)f(x)}{\sqrt{A(x)}}dx, && h<\zeta<1 \\ Y(t)&=\frac{2}{\pi r}\mathrm{Im}\int_0^{x_\zeta}\frac{\left(a\zeta-h\sqrt{a^2+x^2}\right)f(x)}{\sqrt{A(x)}}dx, && \zeta>1 \end{aligned} \tag{B45}$$

For the integral involving the Bessel function of the second order, we have:

$$D(p)=\int_0^\infty xf(x)e^{-p\nu H}J_2(pxr)dx \tag{B46}$$

Instead of using the identities in Eq. (39), we use the following identity for the Bessel function of the second order

$$J_2(z)=J_0(z)+2\frac{d^2J_0(z)}{dz^2} \tag{B47}$$

This results in

$$J_2(pxr)=J_0(pxr)+\frac{2}{p^2x^2}\frac{\partial^2 J_0(pxr)}{\partial r^2} \tag{B48}$$

By the above formula and using Mehler–Sonine representation one may write

$$D(p)=\int_0^\infty xf(x)e^{-pH\nu}J_0(pxr)dx -\frac{4}{\pi}\mathrm{Im}\int_0^\infty ch^2\varphi\, d\varphi\int_0^\infty xf(x)e^{-p(H\nu-irxch\varphi)}dx \tag{B49}$$

The first integral is similar to the case of Bessel of function of the zeros order. For the second integral, we have:

$$\overline{D}(p)=-\frac{4}{\pi}\mathrm{Im}\int_0^\infty ch^2\varphi\, d\varphi\int_0^\infty xf(x)e^{-p(H\nu-irxch\varphi)}dx=\overline{D}_1(p)+\overline{D}_2(p) \tag{B50}$$

Which could be treated with the similar method used for the Bessel function of the zero order, the only difference is the extra factor $ch^2\varphi$. The final results for $\overline{D}_2(p)$ is:

$$\overline{D}_2(p)=0 \qquad \zeta<0$$
$$\overline{D}_2(p)=\frac{4}{\pi Z(1-h^2)}\mathrm{Im}\int_{x_1}^{x_\zeta}\frac{\left(a\zeta-h\sqrt{a^2+x^2}\right)^2 f(x)}{x\sqrt{A(x)}},\qquad \zeta>1 \tag{B51}$$

And for $\overline{D}_1(p)$ we have

$$\overline{D}_1(t)=0, \qquad \zeta<h$$
$$\overline{D}_1(t)=\frac{4}{\pi Z(1-h^2)}\mathrm{Im}\int_0^{m_1}\frac{\left(a\zeta-h\sqrt{a^2-x^2}\right)^2 f(ix)}{x\sqrt{B(x)}}dx,\qquad h<\zeta<1$$
$$\overline{D}_1(t)=\frac{4}{\pi Z(1-h^2)}\mathrm{Im}\int_0^{n_1}\frac{\left(a\zeta-h\sqrt{a^2-x^2}\right)^2 f(ix)}{x\sqrt{B(x)}}dx,\qquad \zeta>1 \tag{B52}$$

Finally from Eqs. (B49), (B50) and (B36) we have

$$D(t)=0, \qquad \zeta<h$$
$$D(t)=\frac{2}{\pi Z}\mathrm{Im}\int_0^{im_1}f(x)\frac{(1-h^2)x^2+2\left(a\zeta-h\sqrt{a^2+x^2}\right)^2}{x\sqrt{A(x)}}dx \qquad h<\zeta<1$$
$$D(t)=\frac{2}{\pi Z}\mathrm{Im}\int_0^{x_\zeta}f(x)\frac{(1-h^2)x^2+2\left(a\zeta-h\sqrt{a^2+x^2}\right)^2}{x\sqrt{A(x)}}dx \qquad \zeta>1 \tag{B53}$$

References

[1] Park J, Kausel E. Response of layered half-space obtained directly in the time domain, part I: SH sources. Bull Seism Soc Am 2006;96(5):1795–809. http://dx.doi.org/10.1785/0120050246.
[2] Kausel E, Park J. Response of layered half-space obtained directly in the time domain, part II: SV-P and three-dimensional sources. Bull Seism Soc Am 2006;96(5):1810–26. http://dx.doi.org/10.1785/0120050247.
[3] Beskos DE. Boundary element methods in dynamic analysis: part II (1986–1996). Appl Mech Rev 1997;50(3):149–97.
[4] Aki K, Richards P. Quantitative seismology. Dey: University Science Books; 1980. p. 11.
[5] Pujol J. Elastic wave propagation and generation in seismology. Cambridge University Press; 2003.
[6] Wolf J, P. Soil–Structure-Interaction Analysis in Time Domain, 07632. Englewood Cliffs, New Jersey: Prentice-Hall; 1988.
[7] Chau K, T. Analytical Methods In Geo-mechanics. Raton Rouge: CRC Press; 2012.
[8] Gazetas G. Analysis of machine foundation vibrations: state of the art. Soil Dyn Earthq Eng 1983;2(1):1–42.
[9] Bhatia KG. Foundations for industrial machines and earthquake effects. ISET J Earthq Technol 2008;45:13–29.
[10] Beskos DE. Boundary element methods in dynamic analysis. Appl Mech Rev 1987;40(1):1–23.
[11] Zhao C. Physical and Chemical Dissolution Front Instability in Porous Media: Theoretical Analyses and Computational Simulations. Heidelberg: Springer; 2014.
[12] Zhao C. Analytical solutions for crack initiation on floor-strata interface during mining. Geomech Eng 2015;8:237–55.
[13] Zhao C. Dynamic and transient infinite elements: theory and geophysical. Geotech Geoenviron Appl 2009 Springer, Berlin.
[14] Zhao C, Hobbs BE, Ord A. Fundamentals of Computational Geoscience: Numerical. Methods Algorithms, vol. 122, 2009, Springer.
[15] Rajapakse RKND, Wang Y. Elastodynamic Green's functions of orthotropic half-plane. J Eng Mech 1991;117(3):588–604.
[16] Wang Y, Rajapakse RKND. Transient fundamental solutions for a transversely isotropic elastic half space. Proc R Soc Lond 1993;442:505–31.
[17] Wang C-Y, Achenbach JD. Elastodynamic fundamental solutions for anisotropic solid. Geophys J Int 1994;118(2):384–92.
[18] Kausel E. Fundamental Solutions in Elastodynamics: A Compendium. Cambridge University Press; 2006.
[19] Pekeries CL, Lifson H. Motion of the surface of a uniform elastic half-space produced by a buried pulse. J Acoust Soc Am 1957;29(11):1233–8.
[20] Pekeris CL. The seismic surface pulse. Proc Natl Acad Sci USA 1955;4:469–80.
[21] Pekeris CL. The seismic buried pulse. Proc Natl Acad Sci USA 1955;41:629–39.
[22] Cagniard L. Reflection and Refraction of Progressive Seismic Wave. McGraw-Hill, International series in the earth sciences; 1939.
[23] Achenbach JD. Wave propagation in elastic solids. Amsterdam, London: North Holland Publishing Company; 1973.
[24] Chao C. Dynamical response of an elastic half-space to tangential surface loadings. J Appl Mech 1960;27(3):559–67.
[25] Jin B, Liu H. exact solution for horizontal displacement at center of the surface of an elastic half space under horizontal impulsive punch loading. Soil Dyn Earthq Eng 1999;18:495–8.
[26] Eskandari-Ghadi M, Pak RYS, Ardeshir-Behrestaghi A. Transversely isotropic elastodynamic solution of a finite layer on an infinite subgrade under surface loads. Soil Dyn Earthq Eng 2008;28(2008):986–1003.
[27] Eskandari-Ghadi M, Ardeshir-Behrestaghi A, Pak RYS, Karimi M, Momeni-Badeleh M. Forced vertical and horizontal movements of a rectangular rigid foundation on a transversely isotropic half-space. Int J Numer Anal Methods Geomech 2012;37:2301–20.
[28] Stoneley R. The seismological implications of aelotropy in continental structures. R Astron Soc Mon Not, Geophys Suppl, Lond, Engl 1949;5:343–53.
[29] Synge JL. Elastic waves in anisotropic media. J Math Phys 1957;35:323–34.
[30] Buchwald VT. Waves in transversely isotropic media. Q J Mech Appl Math 1961;14(4):293–317.
[31] Payton RG. Elastic Wave Propagation in Transversely Isotropic Materials. Dey, 11. Springer; 1961.
[32] Lekhnitskii SG. Theory of Elasticity of an Anisotropic Elastic Body. San Francisco, California: Holden-Day Publishing Co.; 1981.
[33] Eskandari-Ghadi M. A complete solution of the wave equations for transversely isotropic media. J Elast 2005;81:1–19.
[34] Hu HC. On the three dimensional problems of the theory of elasticity of a transely isotropic body. Sci Sin 1953;2:145–51.
[35] Nowacki W. The stress function in three-dimensional problems concerning an elastic body characterized by transverse isotropy. Bull De l 'Acad Pol Sci 1954;2:21–5 Cl. IV.
[36] Wang. MZ, Wang W. Completeness and nonuniqueness of general solutions of transversely isotropic elasticity. Int J Solids Structruct 1995;32:501–13.
[37] Eskandari Ghadi M, Sattar S. Axisymmetric transient waves in transversely isotropic half-space. Soil Dyn Earthq Eng 2009;29:347–55.
[38] Amiri-Hezaveh A, Eskandari-Ghadi M, Rahimian M, Ghorbani-Tanha AK. Impedance functions for surface rigid rectangular foundations on transversely isotropic multilayer half-spaces. J Appl Mech 2013;80:051017-1–12.
[39] Eskandari-Ghadi M, Mirzapour A, Ardeshir-Behrestaghi A. Interaction of rocking vibration of a buried rigid circular disc and a two-layer transversely isotropic half-space. Sci Iran 2013;20(1):1–14.
[40] Zhao C, Hobbs BE, Ord A. Convective and Advective Heat Transfer in Geological Systems. Berlin: Springer; 2008.
[41] Hobbs BE, Ord A, Peng S, Liu L. Inversely-mapped analytical solutions for flow patterns around and within inclined elliptic inclusions in fluid-saturated rocks. Math Geosci 2008;40:179–97.
[42] Hobbs BE, Regenauer-Lieb K, Ord A. Computational simulation for the morphological evolution of nonaqueous-phase-liquid dissolution fronts in two-dimensional fluid-saturated porous media. Comput Geosci 2011;15:2011167–83.
[43] Ord A, Hobbs EB. Analytical solutions of nonaqueous-phase-liquid dissolution problems associated with radial flow in fluid-saturated porous media. J Hydrol 2013;494:96–106.

[44] Eubanks RA, Strenberg E. On the axisymmetric problem of elasticity theory for a medium with transverse isotropy. J Ration Mech 1954;3:89–101.
[45] Chadwick P, Seet TC. Wave propagation in a transversely isotropic heat-conducting elastic material. J Math 1970;17:255–74.
[46] Chadwick P, Shuvalov AL. Bulk-wave polarization fields in transversely isotropic elastic media. Proc R Soc Lond, A 1997;453:77–92.
[47] Khojasteh A, Rahimian M, Eskandari M, Pak RYS. Asymmetric wave propagation in a transversely isotropic half-space in displacement potentials. Int J Eng Sci 2008;46:690–710.
[48] Raoofian Naeeni. M, Campagna R, Eskandari-Ghadi M, Ardalan AA. Performance comparison of numerical inversion methods for Laplace and Hankel integral transforms in engineering problems. Appl Math Comput 2015;250:759–75.
[49] Raoofian Naeeni M, Eskandari-Ghadi M, Ardalan AA, Rahimian M, Hayati Y. Analytical solution of coupled thermoelastic axisymmetric transient waves in a transversely isotropic half-space. J Appl Mech 2012;80:024502–9.
[50] Raoofian Naeeni M, Eskandari-Ghadi M, Ardalan AA, Sture S, Rahimian M. Transient response of a thermoelastic half-space to mechanical and thermal buried sources. ZAMM (Z Angew Math Mech) 2013;95:354–76.
[51] Chadwick P. Wave propagation in transversely isotropic elastic media, I. Homogeneous plane waves. Proc R Soc Lond 1989;422:23–66.
[52] Watson GN. A Treatise on the theory of Bessel function. Cambridge University Press; 1966.
[53] Debnath L, Bhatta D. Integral Transforms and Their Applications. New York: Chapman and Hall; 2007.